7-2024

Post-Fire Sediment Yield From a Central California Watershed: Field Measurements and Validation of the WEPP Model

Amy E. East

Joshua B. Logan

Helen W. Dow

Douglas P. Smith

Pat Iampietro

See next page for additional authors

Authors

Amy E. East, Joshua B. Logan, Helen W. Dow, Douglas P. Smith, Pat Iampietro, Jonathan A. Warrick, Thomas D. Lorenson, Leticia Hallas, and Benjamin Kozlowicz

AGU ADVANCING EARTH AND SPACE SCIENCES

Earth and Space Science

RESEARCH ARTICLE
10.1029/2024EA003575

Post-Fire Sediment Yield From a Central California Watershed: Field Measurements and Validation of the WEPP Model

Amy E. East[1], Joshua B. Logan[1], Helen W. Dow[1], Douglas P. Smith[2], Pat Iampietro[2], Jonathan A. Warrick[1], Thomas D. Lorenson[1], Leticia Hallas[1], and Benjamin Kozlowicz[3]

[1]U.S. Geological Survey Pacific Coastal Marine Science Center, Santa Cruz, CA, USA, [2]College of Science, California State University Monterey Bay, Seaside, CA, USA, [3]AECOM, Inc., Oakland, CA, USA

Abstract In a warming climate, an intensifying fire regime and higher likelihood of extreme rain are expected to increase watershed sediment yield in many regions. Understanding regional variability in landscape response to fire and post-fire rainfall is essential for managing water resources and infrastructure. We measured sediment yield resulting from sequential wildfire and extreme rain and flooding in the upper Carmel River watershed (116 km^2), on the central California coast, USA, using changes in sediment volume mapped in a reservoir. We determined that the sediment yield after fire and post-fire flooding was 854–1,100 t/km^2/yr, a factor of 3.5–4.6 greater than the long-term yield from this watershed and more than an order of magnitude greater than during severe drought conditions. In this first large-scale field validation test of the WEPPcloud/*wepppy* framework for the Water Erosion Prediction Project (WEPP) model on a burned landscape, WEPP predicted 81%–106% of the measured sediment yield. These findings will facilitate assessing and predicting future fire effects in steep watersheds with a Mediterranean climate and indicate that the increasingly widespread use of WEPP is appropriate for evaluating post-fire hillslope erosion even across 100-km^2 scales under conditions without debris flows.

Plain Language Summary In a warming climate, more wildfire and more extreme rain will cause more erosion, producing more sediment that will be carried downstream by rivers. Understanding how much sediment a landscape produces after fire and extreme rain is essential for managing water resources and infrastructure, because sediment fills up storage space in reservoirs and can interfere with proper functioning of water systems and roads. We measured how much sediment was produced in a watershed due to wildfire followed by extreme rain and flooding, studying the Carmel River on the central California coast, USA. We evaluated how much sediment this watershed produced by measuring the volume of sediment deposited within a reservoir that the watershed drains into. We determined that the rate of sediment exported from the study watershed due to a large fire and post-fire floods was much greater than the long-term rate there. Having compared our results with the amount of sediment predicted by a model called the Water Erosion Prediction Project model, we found that the model performed well and realistically predicted the amount of sediment that this landscape would shed. These findings will facilitate assessing and predicting future fire effects in steep watersheds with a Mediterranean-type climate.

Key Points:

- A 116-km^2 central California watershed produced sediment yield of 854–1,100 t/km^2/yr in the first year after a fire and extreme rain
- Post-fire sediment yield in an extremely wet year without debris flows was 3.5–4.6 times greater than the long-term rate
- The Water Erosion Prediction Project model predicted 81%–106% of the measured post-fire sediment eroded from hillslopes

Supporting Information:

Supporting Information may be found in the online version of this article.

Correspondence to:

A. E. East,
aeast@usgs.gov

Citation:

East, A. E., Logan, J. B., Dow, H. W., Smith, D. P., Iampietro, P., Warrick, J. A., et al. (2024). Post-fire sediment yield from a central California watershed: Field measurements and validation of the WEPP model. *Earth and Space Science*, *11*, e2024EA003575. https://doi.org/10.1029/2024EA003575

Received 5 FEB 2024
Accepted 2 JUL 2024

Author Contributions:

Conceptualization: Amy E. East, Douglas P. Smith
Data curation: Joshua B. Logan, Pat Iampietro, Thomas D. Lorenson, Leticia Hallas
Formal analysis: Amy E. East, Joshua B. Logan, Helen W. Dow, Pat Iampietro
Funding acquisition: Douglas P. Smith

1. Introduction

Sediment export from small, steep watersheds responds rapidly to hydroclimatic changes (Lee et al., 2015; Milliman & Farnsworth, 2011; Milliman & Syvitski, 1992; Simpson & Castelltort, 2012) and increases substantially as a result of wildfire (e.g., Florsheim et al., 2017; Moody & Martin, 2009) or major storm rainfall (Barnard & Warrick, 2010; Coats et al., 1985; East et al., 2018; Inman & Jenkins, 1999), and especially from the two processes together (Chin et al., 2019; Keller et al., 1997; Warrick et al., 2022). Future, warmer climate will bring greater wildfire activity and more intense rainfall to many regions, including the western United States (Abatzoglou et al., 2019; Allan & Soden, 2008; Goss et al., 2020; Huang et al., 2020; Intergovernmental Panel on Climate Change, 2014; Jones et al., 2022; Kemter et al., 2021; Melia et al., 2022; Rogers et al., 2020; State of California, 2018; Swain, 2021; Trenberth, 2011; U.S. Global Change Research Program [USGCRP], 2023; Westerling & Bryant, 2008). Therefore, quantifying how fire and extreme rain affect sediment yield is essential to understanding landscape response to modern climate change (East et al., 2022; Singh et al., 2015).

Investigation: Amy E. East, Joshua B. Logan, Douglas P. Smith, Pat Iampietro, Jonathan A. Warrick, Thomas D. Lorenson, Leticia Hallas, Benjamin Kozlowicz
Methodology: Joshua B. Logan, Pat Iampietro
Supervision: Amy E. East
Validation: Helen W. Dow
Writing – original draft: Amy E. East, Joshua B. Logan, Helen W. Dow, Douglas P. Smith, Pat Iampietro
Writing – review & editing: Amy E. East, Joshua B. Logan, Helen W. Dow, Douglas P. Smith, Jonathan A. Warrick

Streamflow, hillslope and channel erosion, and sediment delivery all commonly increase after wildfire owing to loss of vegetation cover and altered soil properties (Cerdà et al., 1995; Cerdà & Lasanta, 2005; DeBano, 2000; DiBiase & Lamb, 2013; Ebel & Moody, 2017; Florsheim et al., 1991; Jackson & Roering, 2009; Lane et al., 2006; Malmon et al., 2007; Rubio et al., 1997; Vieira et al., 2023). Elevated post-fire sediment export can occur as catastrophic debris flows that endanger life and property (e.g., Cannon et al., 2008; Kean et al., 2016; Kean et al., 2019; Kean & Staley, 2021; Ouyang et al., 2023) but also commonly involves overland flow and fluvial transport without debris flows (Moody & Martin, 2009; Rengers et al., 2021; Santi & Rengers, 2020). As fire regimes intensify, it is increasingly important to quantify post-fire landscape change, including sediment export, through spatially explicit measurements that might be applied to better predict landscape response to future fires in the same region. However, direct measurements of post-fire sediment production and transport are uncommon outside of a small number of intensively studied regions (e.g., southern California; DiBiase & Lamb, 2013; Florsheim et al., 2017; Guilinger et al., 2020; Jumps et al., 2022; Kinoshita & Hogue, 2011). Likewise, efforts to model post-fire sediment mobilization have been increasing in number, complexity, and spatial coverage (Ebel et al., 2023; Gartner et al., 2014; Guilinger et al., 2023; Miller et al., 2011; Pelletier & Orem, 2014; Sankey et al., 2017; Wagenbrenner & Robichaud, 2014), but after initial model development, further results and model applications are seldom widely validated against field measurements. Despite the relative rarity of studies comparing post-fire field and model results, the societal benefit of such comparisons is high, including for emergency hazard assessments (Thomas et al., 2023).

Understanding how fire and extreme rain affect sediment yield is critically important for effective 21st-century water and infrastructure security. In addition to water-quality impairment after fire (Basso et al., 2021; Murphy et al., 2023; Paul et al., 2022), greater post-fire sediment runoff can cause excess sedimentation in reservoirs, which eventually could limit water storage capacity in the western U.S. (Belongia et al., 2023; East & Grant, 2023; Goode et al., 2012; Murphy et al., 2018; Randle et al., 2021; Sankey et al., 2017). Additional impacts are occurring to infrastructure and transportation corridors from "nuisance sediment" runoff after fires (Jong-Levinger et al., 2022), increasing maintenance costs and motivating better knowledge of regional fire effects. Similar infrastructure concerns apply to the Mediterranean region, where the fire regime and post-fire erosion are expected to intensify in a warmer climate (García-Ruiz et al., 2013; Morán-Ordóñez et al., 2020). However, the direct impacts of post-fire erosion on sediment yield have not been studied in many places and are often difficult to measure.

This study used reservoir-sedimentation data to measure sediment delivery from a watershed affected by wildfire and extreme hydrologic conditions. Detecting geomorphic change in a reservoir (or a natural lake) is an effective way to measure catchment sediment yield if the water body has enough storage capacity to retain newly delivered sediment rather than passing it downstream, if the dam and reservoir are operated to retain rather than flush sediment, and if the changes in surface elevations are greater than the detection limit of measurement techniques, typically around 10 cm for acoustic and photogrammetric surveys (see East et al., 2021). Where these conditions are met, reservoirs and lakes provide valuable opportunities to measure watershed sediment delivery more reliably than in coastal settings (where waves and currents remobilize and remove sediment) or in-stream sediment-transport measurements (where instruments can be buried or destroyed by post-fire debris flows, or may detect suspended sediment but miss the bed load).

In this paper we use sedimentary deposits in the reservoir behind Los Padres Dam (hereafter informally referred to as "Los Padres reservoir") on the Carmel River, a coastal watershed in central California, to quantify sediment yield for the first year after the 2016 Soberanes Fire. The fire occurred soon after most of California experienced its worst drought in the past millennium during 2012–2015 (Griffin & Anchukaitis, 2014; Hatchett et al., 2015) and was followed immediately by one of the wettest seasons recorded in this region, over winter 2016–2017 (Gershunov et al., 2017). This sequence of extreme events provided an important opportunity to measure sedimentary response to fire and extreme rain in a region expected to receive more of both in a warmer climate. Moreover, the watershed upstream of Los Padres Dam experienced post-fire runoff with no known debris flows in 2016–2017, creating optimal conditions to test the Water Erosion Prediction Project (WEPP) model. WEPP is now the most commonly used process-based model for post-fire runoff and sediment mobilization (Ebel et al., 2023; Lopes et al., 2021). A new online user-interface called WEPPcloud and its associated python framework *wepppy* (Lew et al., 2022; Lew & Srivastava, 2021) facilitate running WEPP and allow users to generate more sophisticated input data, but the output has not been tested extensively in post-fire settings yet. Because WEPP represents hillslope and channel processes, including rill and interrill erosion but not mass

10.1029/2024EA003575

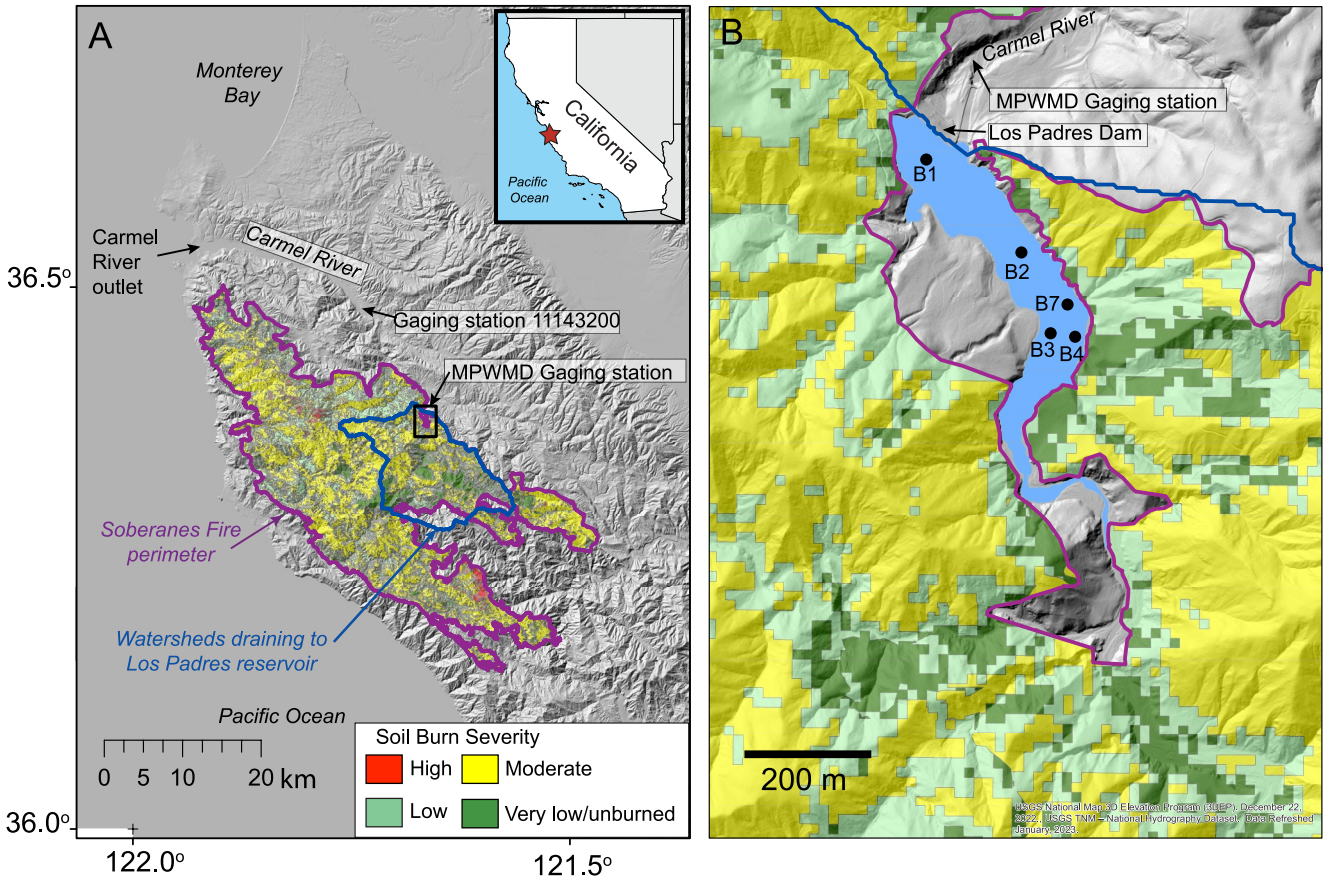

Figure 1. (a). Location map of the general study area, central California coast. Maroon line indicates perimeter of the 2016 Soberanes Fire; area within burn perimeter is color-coded by soil burn severity (mapping from Burned Area Emergency Response Team Report; U.S. Department of Agriculture, 2016). Blue border indicates watershed area draining into the reservoir behind Los Padres Dam; box shows area outlined in panel (b). Two stream-gaging stations are shown: station 11143200, operated by the U.S. Geological Survey (U.S. Geological Survey, 2023), and a station operated by the Monterey Peninsula Water Management District (2023). (b). Detail map of the reservoir behind Los Padres Dam and immediate surrounding terrain, upper Carmel River. Black points within reservoir show locations and names of boreholes. Shaded-relief map underlying (a, b) is the National Map produced by the U.S. Geological Survey's Three-Dimensional Elevation (3DEP) Program (U.S. Geological Survey, 2019).

wasting and debris flows, its performance would be evaluated ideally in a watershed with substantial sediment runoff (i.e., well above field detection capabilities, with a signal clearly exceeding background sedimentation rates) but without debris flows. These conditions were met in the upper Carmel River watershed after the Soberanes Fire. Therefore, our objectives are: (a) to provide quantitative measurements of post-fire sediment yield, information valuable to extrapolating regional response to hydroclimatic extremes and with applications for water management; and (b) to provide field validation of the WEPP model for post-fire erosion in a setting with negligible human impacts and no recent debris-flow activity.

2. Study Area

The Carmel River watershed comprises 650 km^2 of steep terrain (elevation as high as 1,500 m) in the tectonically active Santa Lucia Range, central California coast, discharging into the Pacific Ocean south of Monterey Bay (Figure 1). This study focused on 116 km^2 of the upper Carmel River watershed that drains into Los Padres reservoir, which was impounded by 45-m-high Los Padres Dam in 1949 and had an initial storage capacity of 3.82 million m^3 (3,100 acre-feet; National Inventory of Dams, 2023). The portion of the Carmel River basin upstream of Los Padres Dam is within the Ventana Wilderness area of Los Padres National Forest and is essentially undeveloped with no substantial anthropogenic land use. The terrain includes steep, soil-mantled slopes of fractured, highly weathered granitic and metamorphic bedrock and regolith, covered by predominantly chaparral vegetation with several species of oak trees (Jennings et al., 2010; Smith et al., 2004). Although bedrock lithology and

precipitation vary along the mountains of coastal California, the topography, vegetation, and geomorphic processes (including dry ravel and episodic mass wasting) in this watershed are representative of terrain along ~300 km of the California central coast (Jennings et al., 2010). This region has a Mediterranean climate with warm, dry summers and a wet season from November through March (type "Csb" in the Köppen-Geiger climate classification; Beck et al., 2018). Average annual precipitation in the upper Carmel River basin is 510–630 mm, based on 1981–2010 data (Western Regional Climate Center, 2018). The rainy season in California has become shorter and sharper (more concentrated and with later onset) as the climate warms (Luković et al., 2021).

Fire and post-fire sediment mobilization have long been a concern in the study area. The central California coast region is naturally prone to wildfires, particularly during summer and autumn before the wet season begins. Notably, the Marble Cone Fire of 1977 burned the upper watershed of the Carmel River and much of the surrounding wilderness area. Post-fire erosion in the winter of 1977–1978 delivered more than 685,000 m^3 of sediment into Los Padres reservoir, filling 18% of its storage capacity (U.S. Geological Survey, 1979; Hecht, 1981). Hecht (1981) estimated that sedimentation rates shortly after the Marble Cone Fire were 25 times greater than in the preceding 30 years. A second large dam on the Carmel River, San Clemente Dam, built in the 1920s, 11 km downstream of Los Padres Dam, was removed in 2015 after its reservoir almost entirely filled with sediment, in part d post-fire sedimentation (Harrison et al., 2018). In 2008 the Basin Complex Fire burned much of the same region that the Marble Cone Fire had, including the upper Carmel River watershed, but was followed by a relatively dry water year, in contrast to wet conditions and flooding after the Marble Cone Fire. Warrick et al. (2012) calculated that sediment flux from the Arroyo Seco watershed, immediately southeast of the Carmel River basin, increased 10-fold in the first year after the Marble Cone Fire (relative to non-fire background conditions), shifting the rating curve upward by an order of magnitude, whereas the Basin Complex Fire and subsequent dry winter (2008–2009) caused no substantial change in the rating curve. More recently, small, locally restricted post-fire debris flows occurred in a 2020 burn scar in the lower Carmel River during a 2021 storm, 13 km downstream of Los Padres Dam (Smith et al., 2021).

2.1. Drought, Fire, and Floods, 2012–2017

The Soberanes Fire ignited on 22 July 2016 as a result of an illegal campfire and burned 534 km^2 of the Santa Lucia Range (Figure 1) before being fully contained on 12 October (Monitoring Trends in Burn Severity [MTBS], 2024). At the time, this was the most expensive fire in U.S. history, incurring more than $208 million in management costs, excluding the cost to rebuild any of the 68 buildings destroyed (Potter, 2016). Approximately 80% of the watershed upstream from Los Padres Dam burned, mostly at moderate and low soil burn severity due to the north-facing aspect of most slopes there (Figure 1); south-facing basins had a greater proportion of high soil burn severity (Potter, 2016).

The timing of the Soberanes Fire was bracketed by wet and dry hydrologic extremes. The historic 2012–2015 drought saw 40%–60% of average annual rainfall in this part of the California coast (National Oceanic and Atmospheric Administration, 2024). During those years, annual average flows on the Carmel River ranged from 0.81 to 1.25 m^3/s, well below the 1958–2023 mean of 2.66 m^3/s, and only one flow peak exceeded the 2-year flood magnitude (80 m^3/s). We discuss flow statistics based on records from U.S. Geological Survey (USGS) gaging station 11143200 (U.S. Geological Survey, 2023), 16 km downstream of Los Padres Dam, where the peak-flow record began in 1955. The closest gage to the study area, just downstream of Los Padres Dam, is operated by the Monterey Peninsula Water Management District and began measuring streamflow in 2002. We refer to hydrologic conditions using both gage records where possible but use the longer USGS gage record for evaluating magnitude–frequency relations. The extreme 2012–2015 drought caused substantial tree mortality in some ecoregions, pre-conditioning vegetation for large wildfires (Asner et al., 2015; Littell et al., 2016; Lydersen et al., 2017). Water year 2016 (October 2015 through September 2016) brought near-normal rainfall (National Oceanic and Atmospheric Administration, 2024), although annual flow was still below average in the Carmel River (1.90 m^3/s). Immediately after the Soberanes Fire, water year 2017 (1 October 2016 through 30 September 2017) brought extreme wet conditions along the California coast. Rainfall that winter was 200%–350% of average in the study area and annual average flow on the Carmel River was 7.83 m^3/s, owing to the water vapor delivered by atmospheric rivers having been three standard deviations above the mean (Gershunov et al., 2017). The abnormally wet conditions of 2017 were caused by an unusual weather pattern later named an atmospheric-river "family": repeated storms in close succession comprising highly concentrated vapor transport sustained by tropical heat sources (Fish et al., 2019;

10.1029/2024EA003575

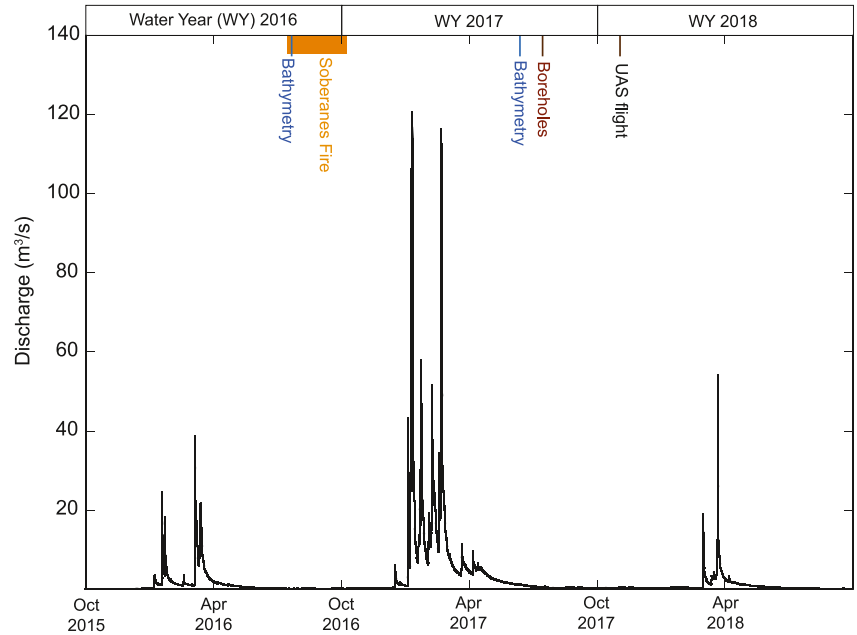

Figure 2. Hydrograph of the Carmel River (15-min resolution) at a gaging station operated by the Monterey Peninsula Water Management District immediately downstream of Los Padres Dam during water years 2016–2018 (1 October 2015 through 30 September 2018). Timing of the Soberanes Fire and collection of data discussed in this paper are shown at top. Data from Monterey Peninsula Water Management District (2023).

Gershunov et al., 2017). In the Carmel River, the extreme rain in winter 2017 led to seven floods (as recorded at USGS gaging station 11143200): two 10-year flood peaks in January 2017, a ~40-year flood (309 m^3/s) in February 2017, and four other 2-year flood peaks (U.S. Geological Survey, 2023; see also East, Harrison, et al., 2023). At the gaging station just below Los Padres Dam, the peak flows reached 106 m^3/s on 8 January 2017, 121 m^3/s on 10 January, and 116 m^3/s on 20 February that year (Figure 2).

Two previous studies have quantified the effects of the extremely wet 2017 winter on sediment discharge from coastal watersheds near the Carmel River. On the San Lorenzo River, a 357-km^2 watershed draining into northern Monterey Bay (unaffected by fires in 2017), nine 2- to 10-year floods that winter, together with landslide activity, led to the 2017 annual sediment load being 10–12 times greater than in an average year and 550 times greater than during the 2012–2015 drought (East et al., 2018). Warrick et al. (2022) estimated that the Big Sur River watershed (151 km^2 in the Santa Lucia Range south of the Carmel River watershed), most of which burned in the Soberanes Fire, produced ~2.2 Mt of sediment—over two orders of magnitude more than in an average water year without fires, and over four orders of magnitude more than during drought conditions in 2013. The massive sediment discharge from the Big Sur River, which widened beaches along the Big Sur coast for years, was attributed to the combination of Soberanes Fire effects and storm rainfall that brought six 2- to 10-year floods in winter 2017 (Warrick et al., 2022).

We use the 2012–2017 drought-fire-flood events in the Carmel River watershed, together with the presence of a sediment-trapping reservoir at Los Padres Dam, as an opportunity to quantify landscape response to a hazard cascade in a watershed where sediment transport is not measured directly and for which no rating curve exists. In doing so we assume that the landscape has enough available sediment supply to emit detectable sedimentary signals of disturbance downstream; with mostly soil-mantled hillslopes, this is not a severely supply-limited landscape. We thereby evaluate how sediment yield from small, steep and relatively undisturbed watersheds in a Mediterranean climate responds to extreme hydroclimatic conditions that are likely to become more common as climate warming progresses (AghaKouchak et al., 2014; USGCRP, 2023), and that have important implications for managing water resources (Basso et al., 2021; Murphy et al., 2018).

3. Methods

This study primarily relied on geomorphic change analyses from bathymetric and topographic data sets collected in Los Padres reservoir. Those analyses of sediment volume change were supplemented by observations of reservoir sediment from boreholes. We then compared field-based estimates of sediment delivered to the reservoir against WEPP model predictions of sediment mass flux from the watershed upstream.

3.1. Geomorphic Change Detection

We used bathymetric and topographic survey data to develop digital surface models (DSMs) of Los Padres reservoir and calculated volume change between successive surveys to analyze sediment deposition. Two geospatial surveys bracketed erosion resulting from the Soberanes Fire and subsequent extreme rain (Figure 2). The first was a single-beam echo-sounder survey on 27 July 2016 by HDR Engineering, Inc., several days after the fire ignited but before any rainfall. That survey utilized a cataraft vessel equipped with a 200-kHz single-beam echo sounder (Teledyne/Odom CVM model) and Trimble R10 antenna for real-time kinematic (RTK) global navigation satellite system (GNSS) geospatial control. Survey control was established using a temporary benchmark on Los Padres Dam with reference coordinates established using a National Geodetic Survey (NGS) Online Positioning User Service (OPUS) solution for the survey date. Subsequent reoccupation of this benchmark, and also a permanent benchmark established in 2008 by California State University Monterey Bay, verified vertical agreement between these marks (HDR Engineering, Inc, 2016).

A second bathymetric survey was completed on 3 June 2017 by California State University Monterey Bay, following the first post-fire wet season with multiple floods on the Carmel River (Figure 2). The 2017 bathymetric data were obtained using a SEA SWATHplus Splash 468 kHz interferometric bathymetric sidescan sonar unit, YSI Castaway CTD and sound-velocity profiler, Applanix POS/MV Wavemaster Inertial Navigation System, and RTK GNSS positioning system mounted on the vessel *R/V Kelpfly*. Survey control was referenced to the permanent benchmark on Los Padres Dam (Smith et al., 2018).

Because sediment accumulation after the Soberanes Fire limited boat access to the upstream portion of the reservoir, the subaerially exposed sediment there was surveyed by an uncrewed airborne system (UAS) operated by the USGS on 1 November 2017 (Figure 2). The survey was conducted using a 3DR Solo quadcopter carrying a Ricoh GR II digital camera triggered at 1 Hz to collect images with 70% spatial overlap along pre-programmed autonomous flight lines 100 m above ground level. Survey control for the UAS flights was established using 20 temporary ground control points consisting of square tarps with black-and-white cross patterns; their locations were measured using RTK GNSS referenced to a base station occupying the permanent benchmark on Los Padres Dam, with reference coordinates established using the NGS OPUS solution for the survey date. We used Structure-from-Motion (SfM) photogrammetric techniques in Agisoft Metashape 1.5.3 to derive a DSM, a digital elevation model (DEM), an orthomosaic image, and a topographic point cloud from the UAS imagery (Logan & East, 2023).

For additional information on recent reservoir sedimentation, we consulted a 2008 swath interferometric sonar survey by California State University Monterey Bay that used the same methods as in the 2017 bathymetric survey (Iampietro, 2024; Smith et al., 2009).

The geospatial data sets were processed in Python using the Rasterio, GDAL, and Numpy libraries, as well as in QGIS, before calculations of volume change (see Figure S1 in Supporting Information S1 for full workflow). The 2016 bathymetric data exhibited a depth-varying vertical offset relative to the 2008 and 2017 surveys. Prior to using the 2016 surface, a vertical adjustment was performed to co-register it to the 2017 surface by identifying locations of minimal vertical change, determined by comparing the 2008 and 2017 surveys (Iampietro, 2024). These locations were used to derive a depth-dependent adjustment function using a least-squares regression analysis (Figure S2 in Supporting Information S1). This adjustment function was then applied to the entire original 2016 bathymetry raster to produce a vertically adjusted 2016 raster, co-registered to the 2008 and 2017 bathymetric rasters for use in the differencing analysis.

We then calculated the volume difference between the 2017 bathymetry and 2016 corrected bathymetry; further co-registration of the surfaces was not necessary, based on a high degree of agreement between the surfaces assessed in a large (9,816 m^2) polygon at the downstream end of the reservoir in an area of expected vertical stability. Because some areas in the 2016 data set showed obvious interpolation artifacts associated with using

single-beam instead of swath sonar over steep slopes in an area with little or no sedimentation (having a low signal-to-noise ratio in the DEM of difference), we calculated 2016–2017 volume change both with and without those artifact-heavy areas. The artifact-rich areas cover 72,300 m^2, or 41.7% of the total surveyed area (171,000 m^2), but their exclusion had little effect on the volume calculations because they occurred not on the main reservoir delta but instead along bedrock-controlled terrain of the lateral, downstream part of the reservoir. Therefore, our interpretations focus primarily on the sediment volume detected in the reservoir delta and thalweg, where the signal-to-noise ratio is high.

Before calculating the volume difference between the 2016 bathymetry and the 2017 UAS SfM data for the upstream end of the reservoir, we co-registered the surfaces by adding 0.281 m to the corrected 2016 bathymetry (adjustment value determined from a polygon on the exposed western shoreline in an area of expected vertical stability near the delta surface that was mapped in both data sets). We then differenced the 2017 UAS-generated surface against the 2016 co-registered, corrected bathymetric surface for the upper end of the reservoir and clipped that region to include only the area not mapped by 2017 sonar bathymetry. This last clipping step, which led to using vertical changes from the 2017 bathymetry instead of those from the UAS data for areas where those data sets overlapped, ensured that sediment reworked after a decrease in lake level between the June bathymetric survey and November UAS survey would be included in the volume calculation, that is, sediment deposited at higher water and then fluvially reworked after late-summer reservoir drawdown is more likely to be accounted for in the volume totals.

We estimated uncertainty in the volume-change calculations using the methods of Anderson (2019). These techniques apply calculations of uncorrelated random error, spatially correlated random error, and systematic error, which are then summed in quadrature. Applications of the Anderson (2019) uncertainty-analysis method to post-fire sediment-volume change in a reservoir based on bathymetric and topographic surveys were described in detail by East et al. (2021); for Los Padres reservoir, we used the same approach as in that study.

3.2. Observations From Borehole Sediment

We supplemented the geomorphic change analyses with observations of Los Padres reservoir sediment recovered in boreholes on 13–17 July 2017 (Figure 1b). These were drilled from a CME-45 barge-mounted drill rig using direct push coring with an Osterberg piston sampler operated by Taber Drilling Company of Sacramento, California, and overseen by AECOM, Inc. Each borehole was drilled to the depth of pre-dam alluvium or bedrock, and sediment was recovered using a split-barrel sampler. Alternate sections were described and sampled; every second section was discarded without examination. Because the drilling operations were intended to characterize general sedimentary properties (with 50% recovery) and not to measure stratigraphy in detail, our opportunistic use of these data is necessarily limited but they provide additional information not evident from the bathymetric surveys.

Grain size and charcoal abundance were analyzed in 42 samples from three of the boreholes, B3, B7, and B2 (in order from upstream to downstream; Figure 1b) at the USGS laboratory in Santa Cruz, California. A sample of surficial sediment from hole B4 was also analyzed. Sediment from these and B1, at the downstream end of the reservoir, was described and logged in the field based on visual observations. To measure grain size, sub-samples weighing 5–50 g were sieved with 1-mm and 0.063-mm sieves to segregate the combined gravel and coarse sand fraction and the mud fraction, respectively. Coarse sand and gravel material was then dry-sieved at quarter-phi intervals and weighed. The remaining sand and mud fractions were analyzed separately on a Beckman Coulter LS 13 20 laser particle-size analyzer (East, Tan, et al., 2023). Charcoal abundance was analyzed in 1.23-ml (quarter teaspoon) sediment samples sub-sampled from the same dried samples from which we measured grain size. The 1.23-ml subsamples were treated with bleach solution for 2 hours while being agitated slowly to remove most non-charcoal organic matter, then wet-sieved, retaining the fraction coarser than 0.125 mm. This fraction was oven-dried at 50°C and examined under a binocular microscope at 15× magnification using a gridded background, and the charcoal particles counted (East, Tan, et al., 2023). This method of counting charcoal abundance in a sample of known volume is based on Anderson et al. (2023), but with subsamples derived from bagged, dried sediment instead of being sampled directly from the core barrel.

3.3. Application of the WEPP Model

The erosion from an undeveloped watershed into a sediment-trapping reservoir after the Soberanes Fire provided an important opportunity to compare field measurements with sediment mass flux predicted by the WEPP model. WEPP is a process-based model that simulates surface and subsurface hydrology and the associated hillslope and channel sediment detachment and transport (Flanagan et al., 2007; Flanagan & Nearing, 1995; Laflen et al., 1991, 1997). WEPP has been used by land managers for decades and tested in numerous post-fire settings (generally at hillslope to plot scale) in which it generally produces satisfactory results though it often underestimates erosion by varying amounts, particularly in regions with high burn severity (Fernández & Vega, 2018; Kampf et al., 2020; Larsen & MacDonald, 2007; Miller et al., 2011; Moffet et al., 2007; Robichaud et al., 2016; Sankey et al., 2017; Spigel & Robichaud, 2007). A recent release of an online interface for WEPP (WEPPcloud; Lew et al., 2022) and an accompanying open-source Python framework for WEPP modeling (*wepppy*; Lew & Srivastava, 2021) greatly facilitates the use of WEPP and the ability to include more sophisticated input data. WEPPcloud and *wepppy* make use of the Natural Resources Conservation Service Soil Survey Geographic Database (NRCS SSURGO/STATSGO2; Reybold & TeSelle, 1989) and the USGS National Land Cover Database (NLCD; Jin et al., 2019) to define soil and land-use inputs to WEPP. Using the "(un)disturbed" module of WEPPcloud/*wepppy*, users also can upload soil burn severity maps and WEPPcloud/*wepppy* automatically modifies the SSURGO/NLCD generated soil properties according to burn severity based on a database of empirical post-fire data (Dobre et al., 2022 and references therein). WEPPcloud/*wepppy* also accesses multiple national gridded climate databases to generate complex rainfall input files for WEPP based on observed weather. WEPP uses daily climate variables from these gridded data sets along with monthly statistics taken from nearby weather stations to generate sub-daily storm characteristics using its built-in synthetic storm generator, CLIGEN.

Although WEPPcloud/*wepppy* has been validated in multiple forested watersheds (Dobre et al., 2022), to date no large-spatial-scale validation of its application to burned watersheds exists. The measurements of post-fire sediment volume made at Los Padres reservoir thus present a rare opportunity to compare field measurements against *wepppy*-generated estimates for >100 km^2 across multiple watersheds, providing a large-scale validation case study that may be useful for future applications of WEPPcloud/*wepppy* to post-fire scenarios. We ran WEPP using the "(un)disturbed" module of *wepppy* on 22 subbasins of the Carmel River watershed that drain into Los Padres reservoir to predict the sediment mass delivered to the reservoir in the first water year following the Soberanes Fire. These 22 watersheds ranged in size from 0.15 to 44 km^2 with relief ranging from 278 to 1170 m. We used a soil burn severity map for the Soberanes Fire generated by the Burned Area Emergency Response Team (U.S. Department of Agriculture, 2016) that split the landscape into categories of low burn severity, moderate burn severity, high burn severity, and unburned. (See also the Soberanes Fire Watershed Emergency Response Team Report; California Department of Forestry and Fire Protection [CalFire], 2016.) We used the 2013 version of the National Land Cover Database for land cover as it was the most recent version prior to the Soberanes Fire.

Sensitivity analyses using the WEPP model have found that predicted post-fire erosion rates are most sensitive to precipitation (Miller et al., 2011). To partially constrain this source of uncertainty in WEPP modeling, we ran WEPP using all the options currently available in *wepppy* for generating climate input files based on observed climate: (a) a 4-km gridded surface meteorological data set called gridMET (Abatzoglou, 2013), (b) gridMET spatially refined using PRISM data (Daly et al., 2008), and (c) a 1-km gridded surface meteorological data set called Daymet (Thornton et al., 2022) that is spatially refined with PRISM data (Daly et al., 2008). We also ran WEPP for these three climate scenarios for the same water year without including the soil burn severity coverage, to estimate sediment yield for the extremely wet water year 2017 in the absence of fire.

For each climate and burn scenario (unburned/burned), we summed all daily estimates for hillslope erosion for each watershed within the first water year following the fire (i.e., water year 2017, from 1 October 2016–30 September 2017). We then summed the WEPP-generated sediment mass predictions for all 22 basins and calculated sediment yield based on the modeled area for each scenario. WEPP produces two sediment outputs, both in units of mass: sediment eroded from hillslopes, and sediment delivered to the watershed outlet (a combination of hillslope and channel erosion). Outlet values are applicable only in small watersheds that have no channel storage component, thus this value only includes sediment that is transported to the outlet in one day. We therefore focus on just the aggregated values for hillslope erosion across the 22 watersheds.

4. Results

4.1. Observations From Sediment Deposits

In the first winter after the Soberanes Fire, the high flows on the Carmel River (Figure 2) brought large quantities of sediment into Los Padres reservoir (Figure 3). Sediment mobilized from the upper watershed apparently through hillslope and fluvial processes, with no known debris flows. Our observations from walking along the Carmel River channel for ~200 m upstream of the reservoir in June and July 2017 yielded no sign of recent debris-flow deposits into the reservoir, only sand and gravel fluvial deposits and burned wood. Several fresh overland-flow channels were present on slopes above the reservoir (Figure 3c) but no true debris flows and no deep-seated landslides were observed.

The combination of surficial mapping and borehole data allowed us to characterize the extent and composition of newly deposited post-fire sediment. The deposit from winter 2017 locally exceeded 4 m thick in the uppermost reservoir delta (Figures 4 and 5). Along the upstream 250 m of the delta, the newly aggraded topset strata were slightly above the maximum water-surface elevation of the reservoir (full pool) as controlled by Los Padres Dam (Figure 5), presumably deposited in a backwater zone during Carmel River flooding. Thickness of the new deposit decreased with distance downstream (Figures 4 and 5) as the reservoir sediment exhibited "Gilbert delta" morphology, with topset, foreset, and bottomset beds (Figure 5). The 2017 bathymetric survey showed the new sediment to be 32 cm thick at borehole site B3 on the delta foreset. This newly deposited material was 53% sand with the rest silt and clay, and contained abundant vegetation debris (Figures S2 and S3 in Supporting Information S1; East, Tan, et al., 2023). Organic material was abundant generally; the new deposit was 44 cm thick at site B4 and 50 cm thick at site B7, both on the delta foreset, and at those sites the new, uppermost material was also organic-rich (containing grass, leaves, and rootlets). The surficial sediment at site B7 was 79% sand. At site B2, farther downstream near the foreset-bottomset transition, new deposition in 2017—very soft, organic-rich black mud—was 32 cm thick, with twigs and other organic matter. The uppermost sediment at B2 (Figure 3d) was finer than at the upstream boreholes, containing more than 90% silt and clay (Figure S3 in Supporting Information S1). At bottomset site B1 new deposition was essentially not detected in the bathymetric surveys (Figures 4 and 5) and any new surficial material was visually indistinguishable from underlying sediment (essentially all of B1 contained homogenous black mud; Figure S2 in Supporting Information S1). Below the apparent 2017 fire-and-flood sediment, the reservoir delta contained heterogenous grain sizes and, again, abundant organic matter. Sand dominated most borehole profiles. At site B3 most samples had 50%–90% sand and median grain sizes were very fine to fine sand (between 0.05 and 0.2 mm). Site B7 was similar, dominated by very fine sand (sand percentages commonly 20%–85% and D_{50} values mostly greater than 0.05; Figure S3 in Supporting Information S1). Several samples from each borehole contained gravel (Figure 3e, Figures S2 and S3 in Supporting Information S1). These sedimentological parameters provided a basis for converting volume estimates to mass (next section) although density was not measured directly in borehole material.

Charcoal abundance generally increased with distance downstream in the reservoir delta. Samples from borehole B3 contained less than 100 charcoal particles per 1.23-ml sample, with values ranging from 2 to 98 (mean of 30) and the topmost (2017) layer having 72. At site B7 the topmost sediment was not sampled, but the top of B4 had a charcoal count of 172 and two other samples at depths of several meters (older than 2017) contained more than 100 particles. At site B2, 300 m downstream of B7, the topmost sample had only 15 charcoal fragments but samples with hundreds of charcoal particles occurred deeper in that core (Figure S3 in Supporting Information S1). A sample from 465 cm below the lakebed in core B2, about one third of the sediment thickness above the pre-dam valley floor, contained 1856 charcoal fragments, the most of any sample we analyzed; we surmise that this horizon reflected the 1977 Marble Cone Fire. The increase in charcoal abundance downstream is consistent with charcoal having lower density than siliciclastic sediment, thus tending to settle out of the river plume in the more quiescent, downstream reservoir region rather than over the delta topset. These opportunistic analyses provide additional insights into the character and distribution of post-fire sediment deposition to inform future studies that may use reservoir deposits to examine landscape responses to extreme events.

4.2. Calculations of Sediment Volume, Mass, and Yield

Based on the geomorphic change detection using the bathymetric sonar and UAS SfM data sets in the reservoir delta and thalweg, the Los Padres reservoir sediment volume increased by 70,788 ± 5,604 m^3 between 2016 and 2017—rounding to three significant figures, 70,800 ± 5,600 m^3 (Table 1; Figure 4). Of this amount,

10.1029/2024EA003575

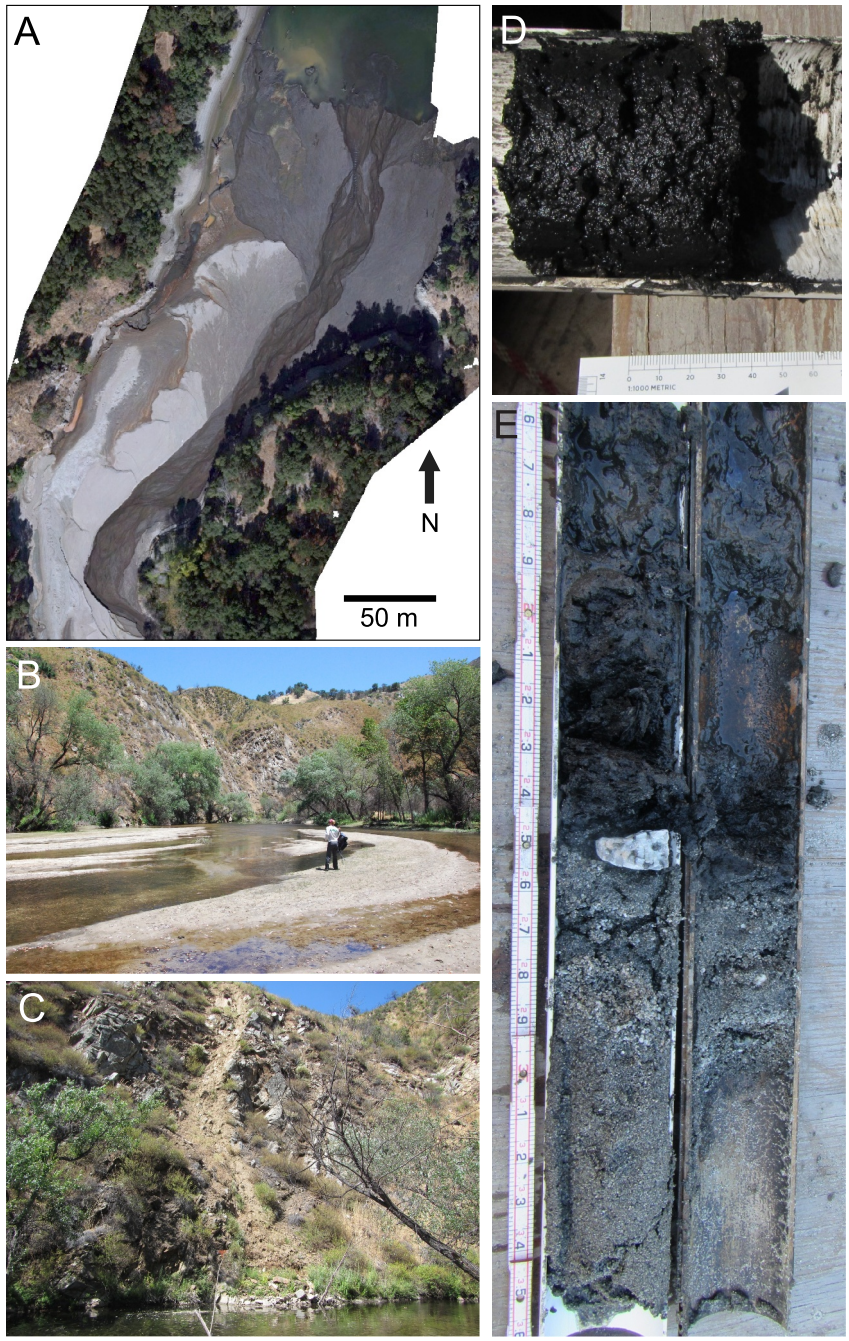

Figure 3. Field photographs from the reservoir behind Los Padres Dam (informally, "Los Padres reservoir") several months after major post-fire runoff, 2017. (a) Aerial orthomosaic image obtained from UAS flight on 1 November 2017, showing the upper part of the reservoir including subaerially exposed sand and gravel deposited in winter 2017. The newly deposited sediment in the region shown in panel (a) was 3–4 m thick. (b) Oblique view of the sediment deposit shown in panel (a), at the upstream (southern) end of Los Padres reservoir, viewed facing upstream. (c) View of a steep slope at the upstream end of Los Padres reservoir (immediately upstream of the location in [a and b]) showing evidence of recent overland flow; a gully approximately 2 m wide is visible in the center of the image. (d) Muddy, organic-rich sediment, presumably deposited in winter 2017, from the top of borehole B2. (e) Sediment recovered from depths of 460–500 cm in borehole B3 (below the limit of new 2017 deposition), showing examples of the variable grain size in the upper Los Padres reservoir delta: predominantly mud at top of image, pebble in center, and medium to coarse sand toward bottom of image.

10.1029/2024EA003575

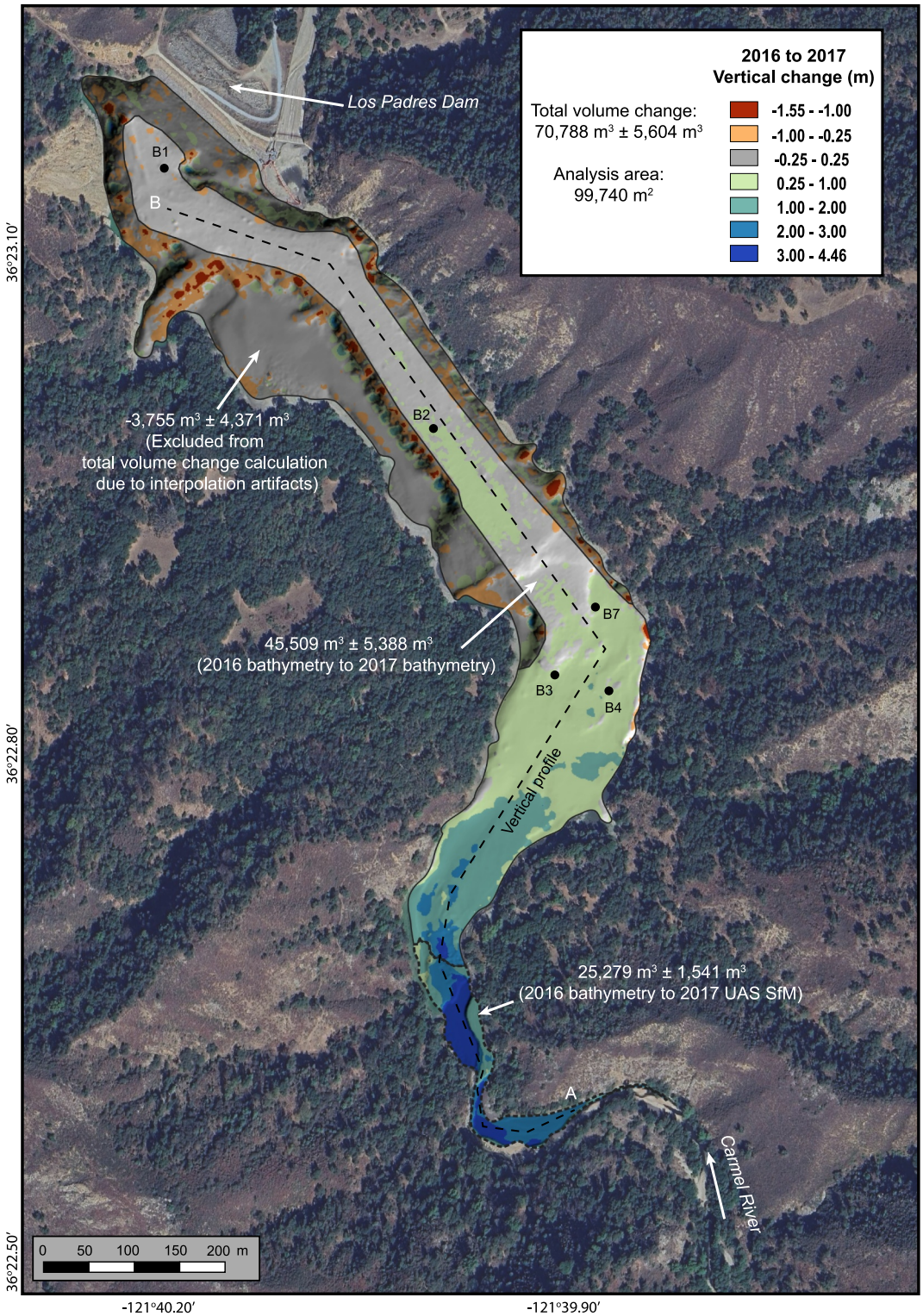

Figure 4. Results of geomorphic change detection analysis of sediment volume differences between 2016 and 2017. The large, lightly shaded region shows the area used for final estimate of volume change (see Figure S1 in Supporting Information S1 for workflow). The darkly shaded region delineates the excluded areas on bedrock-controlled terrain outside of the main reservoir delta where interpolation artifacts (in red) are prevalent. That excluded area, with a low signal-to-noise ratio due to little or no sedimentation, appeared unchanged between 2008 and 2017 (if included, it would lower the volume-change estimate by 5%). Dashed line shows the location of the longitudinal profile plotted in Figure 5. Black points show borehole locations. Background image from October 2022, accessible from Google Earth.

45,509 ± 4,371 m^3 resulted from differencing the DEMs from the bathymetric sonar surveys in 2017 and 2016, and another 25,279 ± 1,541 m^3 was detected at the upstream end of the reservoir by differencing the 2017 UAS SfM-generated surface against the 2016 bathymetric survey (Table 1; Figure 4 and Figure S1 in Supporting Information S1). As discussed in Section 3.1, our best estimate of volume change excluded areas outside of the delta and thalweg where interpolation artifacts were abundant in the DEM of difference, resulting from comparison of two different types of sonar data in areas with a low sedimentation signal-to-noise ratio and steep slopes. That excluded area appeared unchanged between the 2008 and 2017 surveys; if included, it would reduce our volume estimate by 5% (Figure 4).

Our best estimate of volume change, 70,800 ± 5,600 m^3, is conservative because it does not include a small area at the upstream part of the reservoir that was imaged in the 2017 UAS survey but not by boat in 2016, as the 2016 survey only included the thalweg. Some post-fire sediment appeared (visually) to have deposited outside of the channel in an apparent backwater zone in 2017, an area of approximately 200 m^2 where no 2016 data existed for comparison, upstream of the location marked "A" on Figure 4. Deposition in the upstream-most region imaged by both the 2016 sonar and 2017 UAS was 2–3 m thick in the thalweg (Figure 5), so if that thickness was laterally representative, the unmeasured additional deposition could have added as much as 600 m^3 to the total new sediment input.

It is unlikely that our volume estimation missed any other substantial amount of sediment discharged from the watershed above Los Padres Dam. Although some suspended sediment undoubtedly escaped the reservoir during high flows, we can reasonably assume that this was a trivial amount. Surveys of the Carmel River 9 km downstream from Los Padres Dam for a separate study (monitoring a control reach above San Clemente reservoir after the 2015 dam removal) found only isolated, small areas of deposition there in 2017 (Harrison et al., 2018). No substantial deposition occurred there over the next two years either (East, Harrison, et al., 2023).

We used the sediment composition from the boreholes, discussed above, to define reasonable bounds for sediment density in order to convert volume to mass. Most of the 2017 post-fire sediment deposited on the reservoir-delta topset and upper foreset regions, extending ~700 m downstream from the southern limit of the UAS survey (Figure 5). This includes the locations of boreholes B3, B4, and B7 (Figure 4). The sediment from those boreholes was sand-dominated, including the newest material (the upper ~0.5 m). Density of reservoir sediment derived from small, steep watersheds is variable and has not been measured directly in this locality. Therefore, we consulted several references for sediment density of recent fluvial deposits from small, steep watersheds of the western United States. A summary of grain size in 308 samples from two sequential reservoir deltas on the Elwha River, Washington, compiled by Warrick et al. (2015) from four data sets showed that sand-dominated samples had dry bulk density ranging from 830 to 2050 kg/m^3. Warrick et al. (2015) found that the mean dry bulk density of the sand-dominated samples in the upper reservoir there ranged from 1420 to 1760 kg/m^3 among three data sets. Based on those findings, we assumed a range of 1400–1800 kg/m^3 for the Los Padres reservoir material. This is consistent with the 1600 kg/m^3 that Best and Griggs (1991) assumed when calculating a regional budget for littoral sediment derived from central California watersheds. Given the short time elapsed between the new sediment deposition and bathymetric data collection, we do not factor in possible effects of compaction. Using 1,400–1,800 kg/m^3, our calculated volume change corresponds to a mass of 99,100 ± 7,850 tonnes (t) if the density is 1,400 kg/m^3, or 127,000 ± 10,100 t if the density if 1,800 kg/m^3. Given the contributing watershed area of 116.1 km^2, the sediment yield over winter 2017 is estimated to be 854 ± 67.6 t/km^2/yr for a density of 1,400 kg/m^3, and 1,100 ± 86.9 t/km^2/yr for a density of 1,800 kg/m^3.

We also calculated the sediment volume difference between the 2008 and 2016 bathymetric surfaces. The 2008–2016 values are an underestimate because the 2008 data set did not include ~20,000 m^2 of the reservoir delta region, not surveyed due to shallow water; there was a small amount of net aggradation (~1–1.5 m) on the delta upstream of the unsurveyed region (Figure 5). Using the available 2008 and 2016 data yielded a volume change of 18,700 ± 5,730 m^3 (rounding to three significant figures; Table 1). That equates to a mass of 26,100 ± 8,020 t if the density is 1,400 kg/m^3 and 33,600 ± 10,300 t if the density is 1,800 kg/m^3. Annualizing over the eight years between those surveys, which included the historic 2012–2015 drought, the sediment yield for that time interval is estimated to have been ~28.1–36.2 t/km^2/yr.

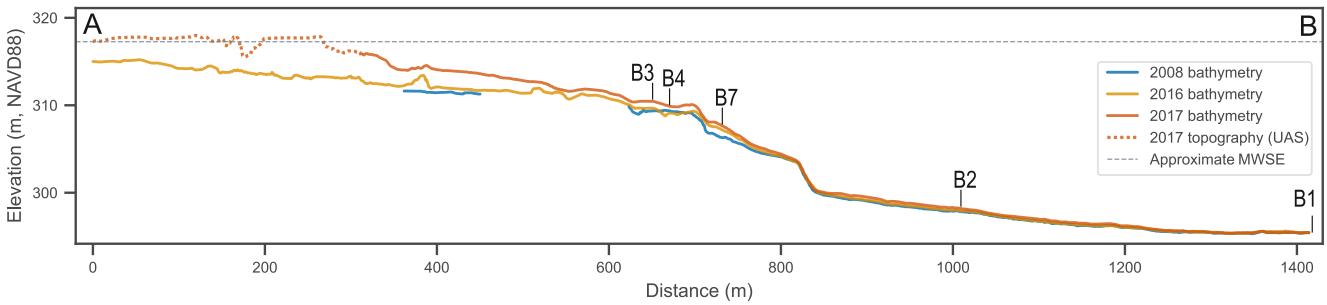

Figure 5. Longitudinal profiles along the sediment surface behind Los Padres Dam (dashed line in Figure 4), showing sediment surface elevations in 2016 (orange line) and 2017 (red line, solid for bathymetric survey and dashed for UAS topographic survey data). Elevations are relative to the NAVD88 vertical datum. The 2008 survey is also shown for reference, although its coverage was incomplete at the upstream end of the reservoir (blue line). Gray, horizontal dashed line shows the water surface when the reservoir is at full pool, 317.27 m (maximum water surface elevation, MWSE). Locations of boreholes (projected onto profile) are shown with vertical black lines.

4.3. Results From WEPP Model Runs

The WEPP model runs for the watershed area above Los Padres Dam during water year 2017, using the soil burn severity coverage from the Soberanes Fire, predicted hillslope erosion of 65,100–102,000 t (rounded values). This corresponds to modeled sediment yield of 579–903 t/km^2/yr for the extremely wet year immediately after the fire. The lowest modeled erosion estimate of 65,100 t (yield 579 t/km^2/yr) came from the climate scenario that used the gridded meteorological data set Daymet with PRISM spatialization, whereas using either of the two gridMET scenarios produced higher values: 100,604 t (895 t/km^2/yr) with gridMET alone, and 101,505 t (903 t/km^2/yr) using gridMET with PRISM data. Thus, the standalone gridMET scenario and the gridMET with PRISM spatialization climate scenario produced very similar results (within 1% of each other), although the results from the 22 watersheds are not significantly different between any three of the climate scenarios ($p >> 0.05$ in paired t-tests).

Comparing these model results against the field-based sediment-mass estimates (Section 4.2, above), both gridMET results are substantially closer to the measured value. With these gridMET results as our preferred range (Table 2), WEPP predicted 81.4%–82.1% of the sediment mass when a density of 1,800 kg/m^3 is assumed for the reservoir deposit, and 105%–106% of the sediment mass calculated using a density of 1,400 kg/m^3. Separate runs of the WEPP model using the two gridMET climate scenarios but excluding the burn-severity map, that is, predicting hillslope erosion for the same hydrologic conditions of water year 2017 but if the Soberanes Fire had not occurred, indicates a sediment mass of 37,700–43,000 t and sediment yield of 336–382 t/km^2/yr. Therefore, WEPP predicted unburned sediment yield that was 37.5%–42.3% of the WEPP-derived yield for the burned case, and 30.5%–44.8% of the observed, field-derived sediment yield from the burned landscape, depending on the assumed density (Table 2).

Table 1
Changes in Reservoir Deposits Behind Los Padres Dam, Including Sediment Volume Between 2016 and 2017, Estimated to 95% Confidence Level From Geomorphic Change Detection Using Bathymetric and UAS Topographic Data

DEM differencing region	Total net volume difference (m^3)	Total volumetric uncertainty (m^3)	Measurement area (m^2)	Uncorrelated random error (m^3)	Spatially correlated random error (m^3)	Systematic error (m^3)
2016 bathymetry (depth-corrected) to 2017 bathymetry	45,509	± 5,388	90,294	± 45	± 803	± 5,327
2016 bathymetry (depth-corrected and co-registered to UAS data) to 2017 USA topography	25,279	± 1,541	9,446	± 29	± 297	± 1,511
Total	**70,788**	**± 5,604**	99,740			
2008 bathymetry to 2016 bathymetry (depth-corrected)	18,657	± 5,727	68,325	± 48	± 1,474	± 5,534

Note. Volume difference between the 2008 and 2016 surfaces was also calculated for reference. Uncertainty estimation used the methods of Anderson (2019). Where these values are discussed in the text, they have been rounded to three significant figures, following convention.

Table 2
Summary of Sediment Yield (in t/km^2/yr) From the Upper Carmel River Watershed, California, Above Los Padres Dam, Calculated for Different Time Intervals and With Various Methods

	Sediment yield (t/km^2/yr)
Water-year 2017, after Soberanes Fire and Extreme rain (this study, field measurements)	**854–1,100**
Water-year 2017, after Soberanes Fire and extreme rain (this study, WEPP model estimate)	**895–903**
Yield from sediment export after 1977 Marble Cone Fire and 1978 wet year (Hecht, 1981)	8,260–10,600
WEPP estimate for water-year 2017 without Soberanes Fire (this study)	**336–383**
Annualized yield between 2008 and 2016 (this study; includes historic drought)	**28.1–36.2**
Annualized yield for 1949–2017 (Smith et al., 2018)	225–290
Long-term yield from entire Carmel River watershed, from ^{10}Be data (Young & Hilley, 2018)	241

Note. Rows in bold text represent findings from this study. The WEPP values shown used the two scenarios with gridMET climate parameterization. Uncertainty ranges reported for field data are based on assumptions of sediment density in volume-to-mass conversions. The 2008–2016 values are an underestimate because the 2008 bathymetric data set did not include ~20,000 m^2 of the reservoir delta region, not surveyed due to shallow water.

Although we have attempted to constrain uncertainty related to climate inputs in WEPP, it is possible that the combination of these gridded data sets and the synthetic storm generator CLIGEN missed smaller-scale precipitation events with locally intense rain that would have an outsized role in post-fire erosion (Oakley, 2021; Oakley et al., 2017). However, the absence of observed debris flows in 2017 above Los Padres reservoir suggests no undetected extremely intense rain bands occurred, and the sum of flow peaks produced by WEPP reproduced the measured streamflow well (Figure S5 in Supporting Information S1). The WEPP estimates of hillslope plus channel erosion are around 1% higher than the hillslope-only values given above; we discuss the hillslope-only values, as explained in Section 3. Additional sources of uncertainty include the interpretations that factor into maps of soil burn severity, and the soil properties assigned within *wepppy* according to land cover, soil type, and burn severity.

5. Discussion

Small, steep watersheds in a tectonically active region, such as the Carmel River, are end members in the spectrum of "reactive" to "buffered" basins described by Allen (2008). Producing high sediment yield but having little or no storage space for sediment deposits, these reactive landscapes respond rapidly to extreme hydroclimatic events, sending sediment to the river outlet or reservoir (if dammed) with little storage in channels or floodplains. The sediment export from such landscapes after fire and flooding can be hazardous to downstream communities, reduces the useful life of reservoirs, or can change coastal morphology, sometimes for years or decades (Warrick et al., 2022, 2023). Understanding these responses is particularly important in our region of interest because California is anticipated to experience 18% greater rain intensity by the late 21st century (Flint & Flint, 2012; Kean & Staley, 2021; Prein et al., 2017), more severe drought (Swain et al., 2018), and larger, more severe fires (Goss et al., 2020; Rogers et al., 2020), all contributing to increasing sediment export (East & Sankey, 2020; McGuire et al., 2024; Sankey et al., 2017). Similar increases in fire and post-fire erosion are anticipated in some other regions beyond the western U.S. as well, particularly the Mediterranean area (McGuire et al., 2024; Morán-Ordóñez et al., 2020). Our findings from the Carmel River watershed provide quantitative information from a cascade of hydroclimatic extremes: the historic 2012–2015 drought (i.e., reduced plant moisture made fuels more easily combustible and weakened or killed trees that stabilize slopes), the 2016 Soberanes Fire, and the 2017 extreme wet season. These results therefore have particular relevance for much of the western U.S. and other regions with similar climate. Although we focus on a field setting with tectonically active terrain (i.e., high sediment yield) and a temperate, Mediterranean-type climate, it is quickly becoming ever more important to understand post-fire geomorphic and sedimentary effects in many types of landscapes and ecoregions, as exceptionally large fires have occurred recently in places where fire activity is accelerating rapidly as climate warms (Jones et al., 2022; Juang et al., 2022): for example, northern boreal forests (Kolden et al., 2024; Rey et al., 2020; Sierra-Hernández et al., 2022; Williams et al., 2020), tundra underlain by permafrost (Holloway et al., 2020; Yanagiya & Furuya, 2020), and the varied ecosystems of Australia and New Zealand (Kemter

et al., 2021; Melia et al., 2022). We note also that being able to detect landscape change using sedimentary deposits downstream from disturbed areas assumes that the sediment supply remains sufficient to generate detectable signals, rather than being severely limited by low rates of bedrock denudation and/or already exhausted by prior natural or anthropogenic disturbances.

We determined that the sediment yield from the upper Carmel River watershed in water year 2017, estimated from our field measurements to be 854–1,100 t/km^2/yr, was more than three times greater than long-term, multidecadal values. This comparison, summarized in Table 2, can be established in two ways: based on the total lost storage capacity of this reservoir since dam completion in 1949, and from published bedrock denudation rates. Using the same 2017 bathymetric survey discussed here, Smith et al. (2018) calculated the remaining water storage volume as the difference between the original full-pool water-surface elevation and the summer 2017 sediment surface. This showed a total storage loss of 1.27 million m^3 over 68 years, or 33% of the original capacity (Smith et al., 2018). Converting that inferred reservoir sediment volume using the same density assumptions we used in Section 4, the resulting multidecadal sediment yield is 226–290 t/km^2/yr. This range is in good agreement with the findings of Young and Hilley (2018) using an entirely different approach. Young and Hilley used cosmogenic ^{10}Be measurements in river sediment samples from 18 watersheds to quantify millennial-scale bedrock denudation rates for most of the Santa Lucia Range. For the Carmel River basin, they determined a denudation rate of 0.091 mm/yr (Young & Hilley, 2018, their Table 1). Assuming a density of 2,650 kg/m^3 for quartz-dominated bedrock, over the 116-km^2 drainage area of interest that vertical denudation rate produces a sediment mass of 241 t/km^2/yr. This rate agrees well with the bathymetry-based estimate over 68 years (Smith et al., 2018). Our 2017 sediment yields are 3.5–4.6 times greater than the Young and Hilley (2018) long-term values. Our inferred 2017 sediment yield is also ∼60 times greater than the annualized rate during drought-dominated years between 2008 and 2016, which in turn were only one-tenth of the Young and Hilley long-term values (Table 2).

Our field-estimated post-fire sediment yield having been 3.5 to 4.6 times greater than the long-term rate represents a relatively small increase compared to most other situations reported in the literature. Post-fire sediment yields can be anywhere from 1.2 to 1,600 times above pre-fire values; one to two orders of magnitude increase is common (McGuire et al., 2024; Owens et al., 2013; Shakesby & Doerr, 2006), as observed also in one northern California study (East et al., 2021). However, some of the higher values in literature examples included situations with post-fire debris flows, not directly comparable with the watershed above Los Padres Dam in 2016–2017.

Notably, post-fire sediment delivery after the 1977 Marble Cone Fire was an order of magnitude greater than after the Soberanes Fire. The Marble Cone Fire also followed severe drought (in 1976–1977) and was succeeded by a wet year with a 10-year flood in January 1978, a hazard sequence considered by Warrick et al. (2012) to have a ∼1,000-year recurrence interval (but repeated only 40 years later, during our study interval). The 685,000 m^3 of lost reservoir storage space in 1978 (Hecht, 1981) corresponds to between 958,000 and 1.23 million t (using density of 1,400–1,800 kg/m^3 again), for an annual yield of 8,260–10,600 t/km^2/yr (Table 2). Without high-resolution meteorological or burn-severity records for 1977–1978, and also considering the lower resolution of the surveying methods used to derive those estimates, we cannot identify precisely why that year's sediment export was so much greater. Field observations in the upper Carmel River watershed in 1977–1978 by Hecht (1981) did not reveal major post-fire debris-flow deposits. It is possible that some debris flows occurred, unobserved, in remote areas farther upstream; this terrain certainly can produce debris flows, as it has after other fires nearby (Smith et al., 2021; Thomas et al., 2023). A more likely reason for the greater response in 1977 than in 2017, however, is that the Marble Cone Fire caused a more severe burn than did the Soberanes Fire. Hecht (1981) observed that the Marble Cone Fire appeared to have burned landscapes severely owing to vegetation having died during the 1976–1977 drought and then tree limbs, weighed down by a rare snow accumulation in 1977, breaking off and remaining on the ground as abundant dead fuel. Fuel loading in this manner might have resulted in a more intense fire or with longer residence time, leading to more severely burned hillslopes able to shed large amounts of sediment during the winter 1978 storms. Additionally, as Cerdà et al. (1995) identified, the high diversity within Mediterranean-type ecosystems results in great spatial variability in soil and vegetation characteristics that locally control fire and post-fire response.

One motivation for this study was its relevance for water-resource management (cf. Hallema et al., 2018). Evaluating sediment delivery using repeat reservoir surveys, rather than alternative methods such as monitoring suspended sediment in streamflow or measuring volume change on individual hillslopes, has the advantages of integrating contributions from both suspended and bedload sediment at a spatial scale large enough to be relevant

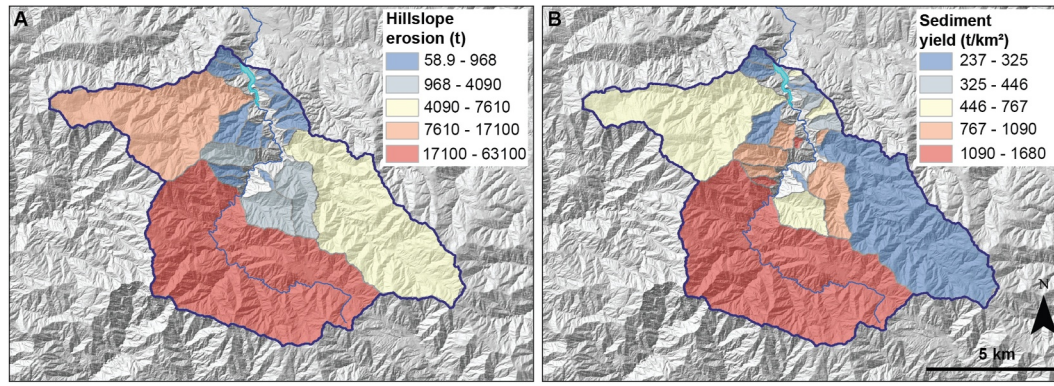

Figure 6. WEPP modeling results for basins that contribute runoff to the reservoir behind Los Padres Dam by (a) sediment mass eroded from hillslopes and (b) sediment yield. Results are shown for the WEPP run using the gridMET climate input without PRISM spatialization. Hillshade map: U.S. Geological Survey (2019).

for reservoir management. In some western-U.S. watersheds, substantial reservoir storage space fills with sediment after just one or two post-fire winter flow seasons. In addition to Los Padres reservoir itself having lost 18% of its capacity after the Marble Cone Fire, other examples include Devil's Gate reservoir in Los Angeles County, California, which essentially filled after the 2009 Station Fire, and nearby Santa Anita reservoir, which experienced rapid sedimentation after the 2020 Bobcat Fire. Sediment has had to be removed from both of those reservoirs, a costly and years-long remediation process (Los Angeles County, 2021, 2023). We find that sediment delivery after the Soberanes Fire caused the loss of approximately 3% of the storage space in Los Padres reservoir. While this is a relatively low proportion, likely owing to moderate and low soil burn severities and the lack of debris flows, the 2016–2017 events still reduced the lifespan of the reservoir more rapidly than the long-term average rates (Table 2). Post-fire sedimentation has contributed significantly to an accelerated consideration of management alternatives for Los Padres Dam and reservoir (AECOM, 2023).

5.1. Performance of the WEPP Model

The Los Padres reservoir sedimentation data afforded a rare opportunity to compare field measurements against WEPP model results (Figure 6). To our knowledge, this is the first field validation of WEPPcloud/*wepppy* in a burned watershed at the order of magnitude spatial scale we have considered. The results indicate good agreement, with *wepppy* run using gridMET-based climate input having predicted ~81.4 to 106% of the measured sediment (the range being primarily a function of density assumptions in the field data). This setting provided a relatively simple, essentially ideal test case, lacking debris flows (WEPP is not designed to represent landslides or debris flows) and with no complicating human land use upstream. In situations with post-fire debris flows, their sediment delivery must be modeled separately (e.g., Gartner et al., 2014).

Compared to previous burned-terrain validation tests using smaller catchments and older versions of the WEPP modeling framework (that used different parameterization of climate, land use and soil burn severity), our larger-scale test using *wepppy* found similar or better model performance. Larsen and MacDonald (2007) compared values from the earlier Disturbed WEPP (Elliott, 2004) against measured sediment volumes trapped from burned hillslope plots and zero-order catchments, finding that the model tended to overpredict sediment yield when measured annualized values were less than 100 t/km^2 (1 Mg/ha, as they reported) and to underpredict when field values were higher than that (by factors of 2–5; Figures 6 and 7 of Larsen & MacDonald, 2007). However, a direct comparison between our results and those of Larsen and MacDonald (2007) is not possible because the plots in their study with yields as high as ours (~900 t/km^2) had high soil burn severity whereas ours were dominantly moderate and low, and their investigation of zero-order catchments in the Rocky Mountains does not have a clear scaling relationship to results from our fourth-order coastal California stream. Working in small (10^{-4} km^2) catchments in Montana, Spigel and Robichaud (2007) measured post-fire sediment yields that were within 15% of the Disturbed WEPP output. Rengers et al. (2021) found that for 0.9–4 km^2 catchments in the high-sediment-yield San Gabriel Mountains, southern California, WEPP predicted only 16% of the post-fire erosion measured with lidar; the relatively poor performance there was attributable to post-fire debris flows, for which WEPP does not

account. Synthesizing field results from eight sites with watersheds 0.01–0.13 km^2 (Robichaud et al., 2008), Robichaud et al. (2016) determined that WEPP (using the ERMiT interface released in 2014) was predicting, on average, 57% of the observed sediment delivery in the first year post-fire. Miller et al. (2011) found a reasonable correlation (R^2 = 0.61) between WEPP-predicted post-fire erosion and those field data, although the predicted rates were much lower than observed rates. In contrast, Kampf et al. (2020) found poor correspondence at the hillslope scale but a good match (within 15%) between measured total hillslope erosion and WEPP model results aggregated across all hillslopes for two watersheds spanning 14 and 16 km^2. Such investigations of model performance in small catchments have supported the widespread use of WEPP, and our addition of a large-scale validation study integrated across 22 sub-watersheds totaling 116 km^2 lends further confidence to the use of this model for post-fire risk assessments on a spatial and temporal scale relevant to reservoir managers.

The large difference between the WEPP-predicted hillslope sediment erosion for water year 2017 with and without the fire (a factor of 2.4–2.7 difference) illustrates the outsized role that fire effects have on hillslope erosion. As mentioned above, post-fire yields are commonly much higher than long-term averages, especially when the fire is immediately followed by a very wet year (Moody et al., 2013; Orem & Pelletier, 2016; Shakesby & Doerr, 2006; Warrick et al., 2012, 2022). Without the fire, the WEPP-predicted sediment yield for the abnormally wet winter of 2017 (336–383 t/km^2/yr; Table 2) is still 39%–59% above the long-term average value, consistent with findings that wet years in this region generate much greater sediment yield even in the absence of fire (Best & Griggs, 1991; East et al., 2018).

WEPP is now the most commonly used model for evaluating post-fire hydrologic and sediment runoff (Ebel et al., 2023; Lopes et al., 2021). WEPP's popularity in U.S.-based research is due to a variety of attributes that make it widely applicable to post-fire research and management questions in the United States and are also why we chose to limit our testing to this particular model. WEPP is a physical post-fire erosion model, which tend to perform better than empirical models that are calibrated to certain locations (Lopes et al., 2021; Pelletier & Orem, 2014), including the Revised Universal Soil Loss Equation (RUSLE; Renard et al., 1997). The availability of national soil and land-cover databases, as well as soil-burn-severity maps for most fires, enables WEPP to be used readily in the United States, though the handling of these input parameters would have to be modified in other regions where such data types are more limited. WEPP can be applied to watersheds as large as ∼50 km^2 while each hillslope is modeled independently at either a 10- or 30-m scale, unlike other commonly used physical models, such as PESERA, which operates at a coarser scale of 1 km (e.g., Kirkby et al., 2008), or ERMiT (Robichaud et al., 2011), which uses WEPP as its underlying processor and is designed to handle smaller spatial scales. Lastly, the new online interface WEPPcloud and python package *wepppy* (Lew et al., 2022; Lew & Srivastava, 2021) facilitate preparing input data to generate site-specific parameters such as topography, land cover, and historical weather, and will likely contribute to the increased use of WEPP by U.S.-based scientists. Our results suggest that WEPPcloud/*wepppy* performs satisfactorily (predicting 81.4%–106% of the measured sediment quantity) with these site-specific attributes but otherwise default parameters in post-fire settings without debris flows.

6. Conclusions

This study analyzed sediment yield from a central California watershed after a cascading hazard sequence: drought, fire, and floods. The increase in especially fire and intense rain as climate warms will lead to greater watershed sediment yields, and field studies such as this are essential for understanding landscape responses to hydroclimatic hazard cascades. Repeated surveys of sediment in lakes or reservoirs, coupled with core or borehole stratigraphy, can prove valuable for quantifying downstream responses to changing watershed conditions. Lake deposits provide the advantage of reflecting both suspended and bed-load sediment delivery from multiple upstream catchments and are often easier to measure than fluvial sediment transport, especially where long-term records are desired (cf. Anderson & Wahl, 2016; East et al., 2022; Snyder et al., 2006; Thurston et al., 2023).

From surveying reservoir deposits behind Los Padres Dam, we find that post-fire sediment yield from the upper Carmel River watershed during an extremely wet winter immediately after the Soberanes Fire, in 2016–2017, was 854–1,100 t/km^2/yr. This represents a factor of 3.5–4.6 increase over the long-term average yields from this watershed, and more than an order of magnitude above recent historic drought conditions. In the first large-scale field validation test of WEPPcloud (*wepppy*) in a burned area (simplified by the lack of debris flows or recent human land use), the model predicted 81.4%–106% of the measured sediment yield. WEPP also predicted that

without the fire, the wet winter alone would have elevated sediment yield by 39%–59% above the long-term values.

Post-fire flooding can reduce reservoir storage capacity due to excess sediment delivery. This is evident in the reservoir behind Los Padres Dam, where the loss of 33% of the original storage volume since 1949 is primarily attributable to post-fire sedimentation: 3% of total capacity was lost in the first winter after the Soberanes Fire (this study) and 18% was lost shortly after the 1977 Marble Cone Fire. In this and other reservoirs, such proportionally large capacity loss can necessitate costly, long-term mitigation to ensure water security. By quantifying post-fire sediment yield and estimating the extent to which this departs from background conditions, field and modeling studies such as these provide information essential to water-resource managers. Post-fire sediment yields vary widely with terrain, hydrology, ecology, and fire conditions, and collecting data from a large number of case studies will be essential to support land- and water-management decisions in the coming decades. Because the terrain in the Carmel River basin is similar to much of coastal California, these results facilitate assessing future fire effects in this region and landscape type. We encourage additional field and modeling studies to continue expanding the range of conditions informing expectations of post-fire response.

Data Availability Statement

All data discussed in this paper are publicly available. Bathymetric survey data can be downloaded from Iampietro (2024). The UAS imagery collected from the upper reservoir behind Los Padres Dam in 2017 can be downloaded from Logan and East (2023). Sediment grain-size and charcoal abundance data are available from East, Tan, et al. (2023). Additional data on lead and cesium isotope activity in the borehole samples are shown in the Supporting Information and are available from Lorenson and East (2024). The version of WEPP used in this study, *wepppy*, is an open-source model available from Lew and Srivastava (2021), and additional documentation about calibration and sensitivity of the WEPP model is available from https://doc.wepp.cloud/FAQ.html. The fire-perimeter and burn-severity data for the Soberanes Fire are available for download from https://mtbs.gov/. Streamflow data from the Carmel River below Los Padres Dam can be obtained from the Monterey Peninsula Water Management District (MPWMD) through the portal at: https://map.mpwmd.net/?page=map or, for older archived data, by written request to MPWMD. Data from USGS gaging station 11143200 (Carmel River at Robles del Rio) are from U.S. Geological Survey (2023; available at https://waterdata.usgs.gov/monitoring-location/11143200).

Acknowledgments
This study was supported by the U.S. Geological Survey (USGS) and by California State University Monterey Bay (CSUMB) through their funding agreement with the Monterey Peninsula Water Management District (MPWMD). The authors gratefully acknowledge collaboration with Rikk Kvitek of CSUMB on the collection of bathymetric data. We appreciate the observations of the Marble Cone Fire and 1977–1978 winter in the upper Carmel River watershed shared by Barry Hecht of Balance Hydrologics. We thank Lysanna Anderson and David Wahl (USGS Geology, Minerals, Energy, and Geophysics Science Center) for generous guidance on measuring charcoal abundance in the laboratory and studying fire records in lacustrine deposits. Matthew Malkowski (now at University of Texas, Austin) assisted with the UAS data collection. Angela Tan oversaw laboratory grain-size analysis at the USGS Pacific Coastal and Marine Science Center. Larry Hampson of MPWMD provided background information on the history of Los Padres Dam operations; Cory Steinmetz of MPWMD provided discharge data for the stream gage below Los Padres Dam. We are thankful to Roger Lew and Mariana Dobre from the University of Idaho for providing substantial support and guidance with running *wepppy*. Discussions with Donald Lindsay (California Geological Survey) and Drew Coe (CalFire) enhanced the authors' understanding of wildfire effects in the study region. We thank Diana Vieira, Joel Sankey, one anonymous reviewer, and editor Cinzia Cervato for their constructive review comments that improved the manuscript. Any use of trade, product, or firm names is for descriptive purposes only and does not imply endorsement by the U.S. government.

References

Abatzoglou, J. T. (2013). Development of gridded surface meteorological data for ecological applications and modelling. *International Journal of Climatology*, *33*(1), 121–131. https://doi.org/10.1002/joc.3413

Abatzoglou, J. T., Williams, A. P., & Barbero, R. (2019). Global emergence of anthropogenic climate change in fire weather indices. *Geophysical Research Letters*, *46*(1), 326–336. https://doi.org/10.1029/2018GL080959

AECOM, Inc. (2023). Los Padres dam and reservoir alternatives and sediment management study. Report prepared for monterey Peninsula water management district in cooperation with California American water, 265 pages with appendices and attachments. Retrieved from https://www.mpwmd.net/wp-content/uploads/Los.Padres.Alts_.Final_.Report.v2-1.pdf

AghaKouchak, A., Cheng, L., Mazdiyasni, O., & Farahmand, A. (2014). Global warming and changes in risk of concurrent climate extremes: Insights from the 2014 California drought. *Geophysical Research Letters*, *41*(24), 8847–8852. https://doi.org/10.1002/2014GL062308

Allan, R. P., & Soden, B. J. (2008). Atmospheric warming and the amplification of precipitation extremes. *Science*, *321*(5895), 1481–1484. https://doi.org/10.1126/science.1160787

Allen, P. A. (2008). Time scales of tectonic landscapes and their sediment routing systems. In K. Gallagher, S. J. Jones, & J. Wainwright (Eds.), *Landscape evolution: Denudation, climate and tectonics over different time and space scales* (Vol. 296(1), pp. 7–28). Geological Society Special Publications. https://doi.org/10.1144/SP296.2

Anderson, L., Presnetsova, L., Wahl, D. B., Phelps, G., & Gous, A. (2023). Assessing reproducibility in sedimentary macroscope charcoal count data. *Quaternary Research*, *111*, 177–196. https://doi.org/10.1017/qua.2022.43

Anderson, L., & Wahl, D. (2016). Two Holocene paleofire records from Peten, Guatemala: Implications for natural fire regime and prehistoric Maya land use. *Global and Planetary Change*, *138*, 82–92. https://doi.org/10.1016/j.gloplacha.2015.09.012

Anderson, S. W. (2019). Uncertainty in quantitative analyses of topographic change: Error propagation and the role of thresholding. *Earth Surface Processes and Landforms*, *44*(5), 1015–1033. https://doi.org/10.1002/esp.4551

Asner, G. P., Brodrick, P. G., Anderson, C. B., Vaughn, N., Knapp, D. E., & Martin, R. E. (2015). Progressive forest canopy water loss during the 2012–2015 California drought. *Proceedings of the National Academy of Sciences*, *113*(2), E249–E255. https://doi.org/10.1073/pnas.1523397113

Barnard, P. L., & Warrick, J. A. (2010). Dramatic beach and nearshore morphological changes due to extreme flooding at a wave-dominated river mouth. *Marine Geology*, *271*(1–2), 131–148. https://doi.org/10.1016/j.margeo.2010.01.018

Basso, M., Mateus, M., Ramos, T. B., & Vieira, D. C. S. (2021). Potential post-fire impacts on a water supply reservoir: An integrated watershed-reservoir approach. *Frontiers in Environmental Science*, *9*, 684703. https://doi.org/10.3389/fenvs.2021.684703

Beck, H. E., Zimmermann, N. E., McVicar, T. R., Vergopolan, N., Berg, A., & Wood, E. F. (2018). Present and future Köppen-Geiger climate classification maps at 1-km resolution. *Scientific Data*, *5*(1), 180214. https://doi.org/10.1038/sdata.2018.214

Belongia, M. F., Wagner, C. H., Seipp, K. Q., & Ajami, N. K. (2023). Building water resilience in the face of cascading wildfire risks. *Science Advances*, *9*(37), eadf9534. https://doi.org/10.1126/sciadv.adf9534

Best, T. C., & Griggs, G. B. (1991). A sediment budget for the Santa Cruz littoral cell, California. In R. H. Osbourne (Ed.), *From shoreline to Abyss* (Vol. 46, pp. 35–50). SEPM Special Publication.

California Department of Forestry and Fire Protection (CalFire). (2016). Soberanes fire watershed emergency response Team report. Report CA-BEU-003422, 29 September 2016 (p. 83). https://www.fire.ca.gov/

Cannon, S. H., Gartner, J. E., Wilson, R. C., Bowers, J. C., & Laber, J. L. (2008). Storm rainfall conditions for floods and debris flows from recently burned areas in southwestern Colorado and southern California. *Geomorphology*, *96*(3–4), 250–269. https://doi.org/10.1016/j.geomorph.2007.03.019

Cerdà, A., Imeson, A. C., & Calvo, A. (1995). Fire and aspect induced differences on the erodibility and hydrology of soils at La Costera, Valencia, southeast Spain. *Catena*, *24*(4), 289–304. https://doi.org/10.1016/0341-8162(95)00031-2

Cerdà, A., & Lasanta, T. (2005). Long-term erosional responses after fire in the central Spanish Pyrenees: 1. Water and sediment yield. *Catena*, *60*(1), 59–80. https://doi.org/10.1016/j.catena.2004.09.006

Chin, A., Solverson, A. P., O'Down, A. P., Florsheim, J. L., Kinoshita, A. M., Nourbakhshbeidokhti, S., et al. (2019). Interacting geomorphic and ecological response of step-pool streams after wildfire. *Geological Society of America Bulletin*, *131*(9–10), 1480–1500. https://doi.org/10.1130/B35049.1

Coats, R., Collins, L., Florsheim, J., & Kaufman, D. (1985). Channel change, sediment transport, and fish habitat in a coastal stream: Effects of an extreme event. *Environmental Management*, *9*(1), 35–48. https://doi.org/10.1007/bf01871443

Daly, C., Halbleib, M., Smith, J. I., Gibson, W. P., Doggett, M. K., Taylor, G. H., et al. (2008). Physiographically sensitive mapping of climatological temperature and precipitation across the conterminous United States. *International Journal of Climatology*, *28*(15), 2031–2064. https://doi.org/10.1002/joc.1688

DeBano, L. F. (2000). The role of fire and soil heating on water repellency in wildland environments: A review. *Journal of Hydrology*, *231–232*, 195–206. https://doi.org/10.1016/s0022-1694(00)00194-3

DiBiase, R. A., & Lamb, M. P. (2013). Vegetation and wildfire controls on sediment yield in bedrock landscapes. *Geophysical Research Letters*, *40*(6), 1093–1097. https://doi.org/10.1002/grl.50277

Dobre, M., Srivastava, A., Lew, R., Deval, C., Brooks, E. S., Elliot, W. J., & Robichaud, P. R. (2022). WEPPcloud: An online watershed-scale hydrologic modeling tool. Part II. Model performance assessment and applications to forest management and wildfires. *Journal of Hydrology*, *127776*, 127776. https://doi.org/10.1016/j.jhydrol.2022.127776

East, A. E., & Grant, G. E. (2023). A watershed moment for western U.S. dams. *Water Resources Research*, *59*(10), e2023WR0356046. https://doi.org/10.1029/2023WR035646

East, A. E., Harrison, L. R., Smith, D. P., Logan, J. B., & Bond, R. M. (2023). Six years of fluvial response to a large dam removal on the Carmel River, California, USA. *Earth Surface Processes and Landforms*, *48*(8), 1487–1501. https://doi.org/10.1002/esp.5561

East, A. E., Logan, J. B., Dartnell, P., Lieber-Kotz, O., Cavagnaro, D. B., McCoy, S. W., & Lindsay, D. N. (2021). Watershed sediment yield following the 2018 Carr fire, Whiskeytown national recreation area, northern California. *Earth and Space Science*, *8*(9), e2021EA001828. https://doi.org/10.1029/2021EA001828

East, A. E., & Sankey, J. B. (2020). Geomorphic and sedimentary effects of modern climate change: Current and anticipated future conditions in the western United States. *Reviews of Geophysics*, *58*(4), e2019RG000692. https://doi.org/10.1029/2019RG000692

East, A. E., Stevens, A. W., Ritchie, A. C., Barnard, P. L., Campbell-Swarzenski, P. L., Collins, B. D., & Conaway, C. H. (2018). A regime shift in sediment export from a coastal watershed during a record wet winter, California—Implications for landscape response to hydroclimatic extremes. *Earth Surface Processes and Landforms*, *43*(12), 2562–2577. https://doi.org/10.1002/esp.4415

East, A. E., Tan, A. C., Hallas, L., & Williamson, J. L. (2023). Grain size and charcoal abundance in sediment samples from Los Padres reservoir, Carmel River watershed, California [Dataset]. *U.S. Geological Survey data release*. https://doi.org/10.5066/P9C7NKM4

East, A. E., Warrick, J. A., Li, D., Sankey, J. B., Redsteer, M. H., Gibbs, A. E., et al. (2022). Measuring and attributing sedimentary and geomorphic responses to modern climate change: Challenges and opportunities. *Earth's Future*, *10*, e2022EF002983. https://doi.org/10.1029/2022EF002983

Ebel, B. A., & Moody, J. A. (2017). Synthesis of soil-hydraulic properties and infiltration timescales in wildfire-affected soils. *Hydrological Processes*, *31*(2), 324–340. https://doi.org/10.1002/hyp.10998

Ebel, B. A., Shephard, Z. M., Walvoord, M. A., Murphy, S. F., Partridge, T. F., & Perkins, K. S. (2023). Modeling post-wildfire hydrologic response: Review and future directions for applications of physically based distributed simulation. *Earth's Future*, *11*(2), e2022EF003038. https://doi.org/10.1029/2022EF003038

Elliot, W. J. (2004). WEPP Internet interfaces for forest erosion prediction. *Journal of the American Water Resources Association*, *40*(2), 299–309. https://doi.org/10.1111/j.1752-1688.2004.tb01030.x

Fernández, C., & Vega, J. A. (2018). Evaluation of the RUSLE and disturbed WEPP erosion models for predicting soil loss in the first year after wildfire in NW Spain. *Environmental Research*, *165*, 279–285. https://doi.org/10.1016/j.envres.2018.04.008

Fish, M. A., Wilson, A. M., & Ralph, F. M. (2019). Atmospheric river families: Definition and associated synoptic conditions. *Journal of Hydrometeorology*, *20*(10), 2091–2107. https://doi.org/10.1175/JHM-D-18-0217.1

Flanagan, D. C., Gilley, J. E., & Franti, T. G. (2007). Water erosion prediction project (WEPP): Development history, model capabilities, and future enhancements. *Transactions of the American Society of Agricultural and Biological Engineers*, *50*(5), 1603–1612. https://doi.org/10.13031/2013.23968

Flanagan, D. C., & Nearing, M. A. (1995). USDA - Water erosion prediction project hillslope profile and watershed model documentation 1. U.S. Department of agriculture. Agricultural Research Service, National Soil Erosion Research Laboratory Report No. 10.

Flint, L. E., & Flint, A. L. (2012). *Simulation of climate change in San Francisco Bay basins, California: Case studies in the Russian river valley and Santa Cruz mountains* (p. 55). U.S. Geological Survey Scientific Investigations Report 2012-5132. Retrieved from https://pubs.usgs.gov/sir/2012/5132/

Florsheim, J. L., Chin, A., Kinoshita, A. M., & Nourbakhshbeidokhti, S. (2017). Effect of storms during drought on post-wildfire recovery of channel sediment dynamics and habitat in the southern California chaparral, USA. *Earth Surface Processes and Landforms*, *42*(10), 1482–1492. https://doi.org/10.1002/esp.4117

Florsheim, J. L., Keller, E. A., & Best, D. W. (1991). Fluvial sediment transport in response to moderate storm flows following chaparral wildfire, Ventura County, southern California. *Geological Society of America Bulletin*, *103*(4), 504–511. https://doi.org/10.1130/0016-7606(1991)103<0504:fstirt>2.3.co;2

García-Ruiz, J. M., Nadal-Romero, E., Lana-Renault, N., & Beguería, S. (2013). Erosion in Mediterranean landscapes: Changes and future challenges. *Geomorphology*, *198*, 20–36. https://doi.org/10.1016/j.geomorph.2013.05.023

Gartner, J. E., Cannon, S. H., & Santi, P. M. (2014). Empirical models for predicting volumes of sediment deposited by debris flows and sediment-laden floods in the transverse ranges of southern California. *Engineering Geology*, *176*, 45–56. https://doi.org/10.1016/j.enggeo.2014.04.008

Gershunov, A., Shulgina, T., Ralph, F. M., Lavers, D. A., & Rutz, J. J. (2017). Assessing the climate-scale variability of atmospheric rivers affecting western North America. *Geophysical Research Letters*, *44*(15), 7900–7908. https://doi.org/10.1002/2017GL074175

Goode, J. R., Luce, C. H., & Buffington, J. M. (2012). Enhanced sediment delivery in a changing climate in semi-arid mountain basins: Implications for water resource management and aquatic habitat in the northern Rocky Mountains. *Geomorphology*, *139–140*, 1–15. https://doi.org/10.1016/j.geomorph.2011.06.021

Goss, M., Swain, D. L., Abatzoglou, J. T., Sarhadi, A., Kolden, C. A., Williams, A. P., & Diffenbaugh, N. S. (2020). Climate change is increasing the likelihood of extreme autumn wildfire conditions across California. *Environmental Research Letters*, *15*(9), 094016. https://doi.org/10.1088/1748-9326/ab83a7

Griffin, D., & Anchukaitis, K. J. (2014). How unusual is the 2012–2014 California drought? *Geophysical Research Letters*, *41*(24), 9017–9023. https://doi.org/10.1002/2014GL062433

Guilinger, J. J., Foufoula-Georgiou, E., Gray, A. B., Randerson, J. T., Smyth, P., Barth, N. C., & Goulden, M. L. (2023). Predicting postfire sediment yields of small steep catchments using airborne lidar differencing. *Geophysical Research Letters*, *50*(16), e2023GL104626. https://doi.org/10.1029/2023GL104626

Guilinger, J. J., Gray, A. B., Barth, N. C., & Fong, B. T. (2020). The evolution of sediment sources over a sequence of postfire sediment-laden flows revealed through repeat high-resolution change detection. *Journal of Geophysical Research: Earth Surface*, *125*(10), e2020JF005527. https://doi.org/10.1029/2020JF005527

Hallema, D. W., Robinne, F.-N., & Bladon, K. D. (2018). Reframing the challenge of global wildfire threats to water supplies. *Earth's Future*, *6*, 772–776. https://doi.org/10.1029/2018EF000867

Harrison, L. R., East, A. E., Smith, D. P., Logan, J. B., Bond, R. M., Nicol, C. L., et al. (2018). River response to large-dam removal in a Mediterranean hydroclimatic setting: Carmel River, California, USA. *Earth Surface Processes and Landforms*, *43*(15), 3009–3021. https://doi.org/10.1002/esp.4464

Hatchett, B. J., Boyle, D. P., Putnam, A. E., & Bassett, S. D. (2015). Placing the 2012–2015 California-Nevada drought into a paleoclimatic context: Insights from walker lake, California-Nevada, USA. *Geophysical Research Letters*, *42*(20), 8632–8640. https://doi.org/10.1002/2015GL065841

HDR Engineering, Inc. (2016). Final Los Padres reservoir survey study report. Technical memorandum delivered to Monterey Peninsula Water Management District, 17 October 2016 (p. 15).

Hecht, B. (1981). Sequential changes in bed habitat conditions in the upper Carmel River following the Marble Cone fire of August, 1977. In R. E. Warner & K. M. Hendrix (Eds.), *California Riparian systems: Ecology, conservation, and productive management* (pp. 135–142). University California Press.

Holloway, J. E., Lewkowicz, A. G., Douglas, T. A., Li, X., Turetsky, M., Baltzer, J. L., & Jin, H. (2020). Impact of wildfire on permafrost landscapes: A review of recent advances and future prospects. *Permafrost and Periglacial Processes*, *31*(3), 371–382. https://doi.org/10.1002/ppp.2048

Huang, X., Swain, D. L., & Hall, A. D. (2020). Future precipitation increase from very high resolution ensemble downscaling of extreme atmospheric river storms in California. *Science Advances*, *6*(29), eaba1323. https://doi.org/10.1126/sciadv.aba1323

Iampietro, P. (2024). Bathymetry of Los Padres reservoir, Carmel, California [Dataset]. https://zenodo.org/records/10582102

Inman, D. L., & Jenkins, S. A. (1999). Climate change and the episodicity of sediment flux of small California rivers. *The Journal of Geology*, *107*(3), 251–270. https://doi.org/10.1086/314346

Intergovernmental Panel on Climate Change (IPCC). (2014). Climate change 2014: Synthesis report. In R. K. Pachauri & L. A. Meyer (Eds.), *Core writing team, contribution of working Groups I, II and III to the fifth assessment report of the intergovernmental panel on climate change* (p. 151). IPCC. Retrieved from https://www.ipcc.ch/report/ar5/syr/

Jackson, M., & Roering, J. J. (2009). Post-fire geomorphic response in steep, forested landscapes: Oregon coast range, USA. *Quaternary Science Reviews*, *28*(11–12), 1131–1146. https://doi.org/10.1016/j.quascirev.2008.05.003

Jennings, C. W., Gutierrez, C., Bryant, W., Saucedo, G., & Wills, C. (2010). *Geologic map of Cailfornia*. California Geological Survey. Geologic Data Map GDM-2.2010, scale 1:750,000. Retrieved from https://ngmdb.usgs.gov/Prodesc/proddesc_96750.htm

Jin, S., Homer, C., Yang, L., Danielson, P., Dewitz, J., Li, C., et al. (2019). Overall methodology design for the United States national land cover database 2016 products. *Remote Sensing*, *11*(24), 2971. https://doi.org/10.3390/rs11242971

Jones, M. W., Abatzoglou, J. T., Veraverbeke, S., Andela, N., Lasslop, G., Forkel, M., et al. (2022). Global and regional trends and drivers of fire under climate change. *Reviews of Geophysics*, *60*(3), e2020RG000726. https://doi.org/10.1029/2020RG000726

Jong-Levinger, A., Banerjee, T., Houston, D., & Sanders, B. F. (2022). Compound post-fire flood hazards considering infrastructure sedimentation. *Earth's Future*, *10*(8), e2022EF002670. https://doi.org/10.1029/2022EF002670

Juang, C. S., Williams, A. P., Abatzoglou, J. T., Balch, J. K., Hurteau, M. D., & Moritz, M. A. (2022). Rapid growth of large forest fires drives the exponential response of annual forest-fire area to aridity in the western United States. *Geophysical Research Letters*, *49*(5), e2021GL097131. https://doi.org/10.1029/2021GL097131

Jumps, N., Gray, A. B., Guilinger, J. J., & Cowger, W. C. (2022). Wildfire impacts on the persistent suspended sediment dynamics of the Ventura River, California. *Journal of Hydrology: Regional Studies*, *41*, 101096. https://doi.org/10.1016/j.ejrh.2022.101096

Kampf, S. K., Gannon, B. M., Wilson, C., Saavedra, F., Miller, M. E., Heldmyer, A., et al. (2020). PEMIP: Post-fire erosion model intercomparison project. *Journal of Environmental Management*, *268*, 110704. https://doi.org/10.1016/j.jenvman.2020.110704

Kean, J. W., McGuire, L. A., Rengers, F. K., Smith, J. B., & Staley, D. M. (2016). Amplification of postwildfire peak flow by debris. *Geophysical Research Letters*, *43*(16), 8545–8553. https://doi.org/10.1002/2016GL069661

Kean, J. W., & Staley, D. M. (2021). Forecasting the frequency and magnitude of postfire debris flows across southern California. *Earth's Future*, *9*(3), e2020EF001735. https://doi.org/10.1029/2020EF001735

Kean, J. W., Staley, D. M., Lancaster, J. T., Rengers, F. K., Swanson, B. J., Coe, J. A., et al. (2019). Inundation, flow dynamics, and damage in the 9 January 2018 Montecito debris-flow event, California, USA: Opportunities and challenges for post-wildfire risk assessment. *Geosphere*, *15*(4), 1140–1163. https://doi.org/10.1130/ges02048.1

Keller, E. A., Valentine, D. W., & Gibbs, D. R. (1997). Hydrological response of small watersheds following the southern California painted Cave fire of June 1990. *Hydrological Processes*, *11*(4), 401–414. https://doi.org/10.1002/(sici)1099-1085(19970330)11:4<401::aid-hyp447>3.0.co;2-p

Kemter, M., Fischer, M., Luna, L. V., Schönfeldt, E., Vogel, J., Banerjee, A., et al. (2021). Cascading hazards in the aftermath of Australia's 2019/2020 Black Summer wildfires. *Earth's Future*, *9*(3), e2020EF001884. https://doi.org/10.1029/2020EF001884

Kinoshita, A. M., & Hogue, T. S. (2011). Spatial and temporal controls on post-fire hydrologic recovery in Southern California watersheds. *Catena*, *87*(2), 240–252. https://doi.org/10.1016/j.catena.2011.06.005

Kirkby, M. J., Irvine, B. J., Jones, R. J. A., Govers, G., & Team, P. (2008). The PESERA coarse scale erosion model for Europe. I. Model rationale and implementation. *European Journal of Soil Science*, *59*(6), 1293–1306. https://doi.org/10.1111/j.1365-2389.2008.01072.x

Kolden, C. A., Abatzoglou, J. T., Jones, M. W., & Jain, P. (2024). Wildfires in 2023. *Nature Reviews Earth & Environment*, *5*(4), 238–240. https://doi.org/10.1038/s43017-024-00544-y

Laflen, J. M., Elliot, W. J., Flanagan, D. C., Meyer, C. R., & Nearing, M. A. (1997). WEPP-Predicting water erosion using a process-based model. *Journal of Soil and Water Conservation*, *52*, 96–102.

Laflen, J. M., Lane, L. J., & Foster, G. R. (1991). WEPP: A new generation of erosion prediction technology. *Journal of Soil and Water Conservation*, *46*, 34–38.

Lane, P. N. J., Sheridan, G. J., & Noske, P. J. (2006). Changes in sediment loads and discharge from small mountain catchments following wildfire in south eastern Australia. *Journal of Hydrology*, *331*(3–4), 495–510. https://doi.org/10.1016/j.jhydrol.2006.05.035

Larsen, I. J., & MacDonald, L. H. (2007). Predicting postfire sediment yields at the hillslope scale: Testing RUSLE and Disturbed WEPP. *Water Resources Research*, *43*(11). https://doi.org/10.1029/2006WR005560

Lee, T.-Y., Huang, C., Jr., Lee, J.-Y., Jien, S.-H., Zehetner, F., & Kao, S.-J. (2015). Magnified sediment export of small mountainous rivers in Taiwan: Chain reactions from increased rainfall intensity under global warming. *PLoS One*, *10*(9), e0138283. https://doi.org/10.1371/journal.pone.0138283

Lew, R., Dobre, M., Srivastava, A., Brooks, E. S., Elliot, W. J., Robichaud, P. R., & Flanagan, D. C. (2022). WEPPcloud: An online watershed-scale hydrologic modeling tool. Part I. Model description. *Journal of Hydrology*, *608*, 127603. https://doi.org/10.1016/j.jhydrol.2022.127603

Lew, R., & Srivastava, A. (2021). rogerlew/wepppy-win-bootstrap. *Zenodo*. https://doi.org/10.5281/zenodo.4902236

Littell, J. S., Peterson, D. L., Riley, K. L., Liu, Y., & Luce, C. H. (2016). A review of the relationships between drought and forest fire in the United States. *Global Change Biology*, *22*(7), 2353–2369. https://doi.org/10.1111/gcb.13275

Logan, J. B., & East, A. E. (2023). Aerial imagery and structure-from-motion data products from a UAS survey of the Los Padres Reservoir delta, Carmel River valley, CA, 2017-11-01 [Dataset]. *U.S. Geological Survey data release*. https://doi.org/10.5066/P9J9CHOH

Lopes, A. R., Girona-García, A., Corticeiro, S., Martins, R., Keizer, J. J., & Vieira, D. C. S. (2021). What is wrong with post-fire soil erosion modelling? A meta-analysis on current approaches, research gaps, and future directions. *Earth Surface Processes and Landforms*, *46*(1), 205–219. https://doi.org/10.1002/esp.5020

Lorenson, T. D., & East, A. E. (2024). Lead, radium, cesium, and thorium isotope activity in sediment samples from Los Padres reservoir, Carmel River watershed, California [Dataset]. *U.S. Geological Survey data release*. https://doi.org/10.5066/P99M6Y8O

Los Angeles County. (2021). Devil's gate reservoir restoration project. Los Angeles County Public Works Department. https://pw.lacounty.gov/swe/DevilsGate/

Los Angeles County. (2023). Santa Anita reservoir post-fire emergency restoration project. Los Angeles county public works department. Retrieved from https://pw.lacounty.gov/wrd/Projects/Bobcatfire/santaanita.shtml

Luković, J., Chiang, J. C. H., Blagojević, D., & Sekulić, A. (2021). A later onset of the rainy season in California. *Geophysical Research Letters*, *48*(4), e2020GL090350. https://doi.org/10.1029/2020GL090350

Lydersen, J. M., Collins, B. M., Brooks, M. L., Matchett, J. R., Shive, K. L., Povak, N. A., et al. (2017). Evidence of fuels management and fire weather influencing fire severity in an extreme fire event. *Ecological Applications*, *27*(7), 2013–2030. https://doi.org/10.1002/eap.1586

Malmon, D. V., Reneau, S. L., Katzman, D., Lavine, A., & Lyman, J. (2007). Suspended sediment transport in an ephemeral stream following wildfire. *Journal of Geophysical Research*, *112*(F2), F02006. https://doi.org/10.1029/2005JF000459

McGuire, L. A., Ebel, B. A., Rengers, F. K., Vieira, D. C. S., & Nyman, P. (2024). Fire effects on geomorphic processes. *Nature Reviews Earth & Environment*, *5*(7), 486–503. https://doi.org/10.1038/s43017-024-00557-7

Melia, N., Dean, S., Pearce, H. G., Harrington, L., Frame, D. J., & Strand, T. (2022). Aotearoa New Zealand's 21st-century wildfire climate. *Earth's Future*, *10*(6), e2022EF002853. https://doi.org/10.1029/2022EF002853

Miller, M. E., MacDonald, L. H., Robichaud, P. R., & Elliot, W. J. (2011). Predicting post-fire hill slope erosion in forest lands of the western United States. *International Journal of Wildland Fire*, *20*(8), 982–999. https://doi.org/10.1071/WF09142

Milliman, J. D., & Farnsworth, K. L. (2011). *River discharge to the coastal ocean: A global synthesis* (p. 385). Cambridge University Press.

Milliman, J. D., & Syvitski, J. P. M. (1992). Geomorphic/tectonic control of sediment discharge to the ocean: The importance of small mountainous rivers. *The Journal of Geology*, *100*(5), 525–544. https://doi.org/10.1086/629606

Moffet, C. A., Pierson, F. B., Robichaud, P. R., Spaeth, K. E., & Hardegree, S. P. (2007). Modeling soil erosion on steep sagebrush rangeland before and after prescribed fire. *Catena*, *71*(2), 218–228. https://doi.org/10.1016/j.catena.2007.03.008

Monitoring Trends in Burn Severity (MTBS). (2024). *Monitoring Trends in burn severity, interagency website maintained by U.S. Department of agriculture*. U.S. Forest Service, U.S. Department of Interior, and U.S. Geological Survey. Retrieved from https://mtbs.gov/

Monterey Peninsula Water Management District. (2023). Data portal for stream flow and rainfall. Retrieved from https://map.mpwmd.net/?page=map

Moody, J. A., & Martin, D. A. (2009). Synthesis of sediment yields after wildland fire in different rainfall regimes in the western United States. *International Journal of Wildland Fire*, *18*(1), 96–115. https://doi.org/10.1071/WF07162

Moody, J. A., Shakesby, R. A., Robichaud, P. R., Cannon, S. H., & Martin, D. A. (2013). Current research issues related to post-wildfire runoff and erosion processes. *Earth-Science Reviews*, *122*, 10–37. https://doi.org/10.1016/j.earscirev.2013.03.004

Morán-Ordóñez, A., Duane, A., Gil-Tena, A., De Cáceres, M., Aquilué, N., Guerra, C. A., et al. (2020). Future impact of climate extremes in the Mediterranean: Soil erosion projections when fire and extreme rainfall meet. *Land Degradation & Development*, *31*(18), 3040–3054. https://doi.org/10.1002/ldr.3694

Murphy, B. P., Yocom, L. L., & Belmont, P. (2018). Beyond the 1984 perspective: Narrow focus on modern wildfire trends underestimates future risks to water security. *Earth's Future*, *6*(11), 1492–1497. https://doi.org/10.1029/2018EF001006

Murphy, S. F., Alpers, C. N., Anderson, C. W., Banta, J. R., Blake, J. M., Carpenter, K. D., et al. (2023). A call for strategic water-quality monitoring to advance assessment and prediction of wildfire impacts on water supplies. *Frontiers in Water*, *5*, 1144225. https://doi.org/10.3389/frwa.2023.1144225

National Inventory of Dams. (2023). Database maintained by the U.S. Army Corps of Engineers [Dataset]. https://nid.sec.usace.army.mil/#/

National Oceanic and Atmospheric Administration. (2024). California Nevada river forecast center, observed precipitation interactive map interface. Retrieved from https://www.cnrfc.noaa.gov/ol.php?type=precip

Oakley, N. S. (2021). A warming climate adds complexity to post-fire hydrologic hazard planning. *Earth's Future*, *9*(7), e2021EF002149. https://doi.org/10.1029/2021EF002149

Oakley, N. S., Lancaster, J. T., Kaplan, M. L., & Ralph, F. M. (2017). Synoptic conditions associated with cool season post-fire debris flows in the Transverse Ranges of southern California. *Natural Hazards*, *88*(1), 327–354. https://doi.org/10.1007/s11069-017-2867-6

Orem, C. A., & Pelletier, J. D. (2016). The predominance of post-wildfire erosion in the long-term denudation of the Valles Caldera, New Mexico. *Journal of Geophysical Research: Earth Surface*, *121*(5), 843–864. https://doi.org/10.1002/2015JF003663

Ouyang, C., Xiang, W., An, H., Wang, F., Yang, W., & Fan, J. (2023). Mechanistic analysis and numerical simulation of the 2021 post-fire debris flow in Xiangjiao catchment, China. *Journal of Geophysical Research: Earth Surface*, *128*(1), e2022JF006846. https://doi.org/10.1029/2022JF006846

Owens, P. N., Giles, T. R., Petticrew, E. L., Leggat, M. S., Moore, R. D., & Eaton, B. C. (2013). Muted responses of streamflow and suspended sediment flux in a wildfire-affected watershed. *Geomorphology*, *202*, 128–139. https://doi.org/10.1016/j.geomorph.2013.01.001

Paul, M. J., LeDuc, S. D., Lassiter, M. G., Moorhead, L. C., Noyes, P. D., & Leibowitz, S. G. (2022). Wildfire induces changes in receiving waters: A review with considerations for water quality management. *Water Resources Research*, *58*(9), e2021WR030699. https://doi.org/10.1029/2021WR030699

Pelletier, J. D., & Orem, C. A. (2014). How do sediment yields from post-wildfire debris-laden flows depend on terrain slope, burn severity class, and drainage basin area? Insights from airborne-LiDAR change detection. *Earth Surface Processes and Landforms*, *39*(13), 1822–1832. https://doi.org/10.1002/esp.3570

Potter, C. (2016). Landscape patterns of burn severity in the Soberanes Fire of 2016. *Journal of Geography & Natural Disasters*, *S6*. https://doi.org/10.4172/2167-0587.S6-005

Prein, A. F., Rasmussen, R. M., Ikeda, K., Liu, C., Clark, M. P., & Holland, G. J. (2017). The future intensification of hourly precipitation extremes. *Nature Climate Change*, *7*(1), 48–52. https://doi.org/10.1038/nclimate3168

Randle, T. J., Morris, G. L., Tullos, D. D., Weirich, F. H., Kondolf, G. M., Moriasi, D. N., et al. (2021). Sustaining United States reservoir storage capacity: Need for a new paradigm. *Journal of Hydrology*, *602*, 126686. https://doi.org/10.1016/j.jhydrol.2021.126686

Renard, K. G., Foster, G. R., Weesies, G. A., McCool, D. K., & Yoder, D. C. (1997). *Predicting soil erosion by water: A guide to conservation planning with the revised universal soil loss equation (RUSLE)* (Vol. 703, p. 494). Department of Agriculture, Agricultural Handbook.

Rengers, F. K., McGuire, L. A., Kean, J. W., Staley, D. M., Dobre, M., Robichaud, P. R., & Swetnam, T. (2021). Movement of sediment through a burned landscape: Sediment volume observations and model comparisons in the San Gabriel Mountains, California, USA. *Journal of Geophysical Research: Earth Surface*, *126*(7), e2020JF006053. https://doi.org/10.1029/2020JF006053

Rey, D. M., Walvoord, M. A., Minsley, B. J., Ebel, B. A., Voss, C. I., & Singha, K. (2020). Wildfire-initiated Talik development exceeds current thaw projections: Observations and models from Alaska's continuous permafrost zone. *Geophysical Research Letters*, *47*(15), e2020GL087565. https://doi.org/10.1029/2020GL087565

Reybold, W. U., & TeSelle, G. W. (1989). Soil geographic data bases. *Journal of Soil and Water Conservation*, *44*, 28–29.

Robichaud, P. R., Elliot, W. J., Lewis, S. A., & Miller, M. E. (2016). Validation of a probabilistic post-fire erosion model. *International Journal of Wildland Fire*, *25*(3), 337–350. https://doi.org/10.1071/WF14171

Robichaud, P. R., Elliot, W. J., & Wagenbrenner, J. W. (2011). Probabilistic soil erosion modeling using the Erosion Risk Management Tool (ERMIT) after wildfires. ISELE Paper Number 11039, presented at the international symposium on erosion and landscape evolution; September 18-21, 2011; Anchorage, AK. ASABE Publication Number 711P0311cd (p. 8). https://www.fs.usda.gov/research/treesearch/41494

Robichaud, P. R., Wagenbrenner, J. W., Brown, R. E., Wohlgemuth, P. M., & Beyers, J. L. (2008). Evaluating the effectiveness of contour-felled log erosion barriers as a post-fire runoff and erosion mitigation treatment in the western United States. *International Journal of Wildland Fire*, *17*(2), 255–273. https://doi.org/10.1071/WF07032

Rogers, B. M., Balch, J. K., Goetz, S. J., Lehmann, C. E. R., & Turetsky, M. (2020). Focus on changing fire regimes: Interactions with climate, ecosystems, and society. *Environmental Research Letters*, *15*(3), 030201. https://doi.org/10.1088/1748-9326/ab6d3a

Rubio, J. L., Forteza, J., Andreu, V., & Cerni, R. (1997). Soil profile characteristics influencing runoff and soil erosion after forest fire: A case study (Valencia, Spain). *Soil Technology*, *11*(1), 67–78. https://doi.org/10.1016/S0933-3630(96)00116-X

Sankey, J. B., Kreitler, J., Hawbaker, T. J., McVay, J. L., Miller, M. E., Mueller, E. R., et al. (2017). Climate, wildfire, and erosion ensemble foretells more sediment in western USA watersheds. *Geophysical Research Letters*, *44*(17), 8884–8892. https://doi.org/10.1002/2017GL073979

Santi, P. M., & Rengers, F. K. (2020). Wildfire and landscape change. *Treatise on Geomorphology*, *13*, 262–287. https://doi.org/10.1016/B978-0-12-818234-5.00017-1

Shakesby, R. A., & Doerr, S. H. (2006). Wildfire as a hydrological and geomorphological agent. *Earth-Science Reviews*, *74*(3–4), 269–307. https://doi.org/10.1016/j.earscirev.2005.10.006

Sierra-Hernández, M. R., Beaudon, E., Porter, S. E., Mosley-Thompson, E., & Thompson, L. G. (2022). Increased fire activity in Alaska since the 1980s: Evidence from an ice core-derived black carbon record. *Journal of Geophysical Research: Atmospheres*, *127*(2), e2021JD035668. https://doi.org/10.1029/2021JD035668

Simpson, G., & Castelltort, S. (2012). Model shows that rivers transmit high-frequency climate cycles to the sedimentary record. *Geology*, *40*(12), 1131–1134. https://doi.org/10.1130/G33451.1

Singh, A., Reinhardt, L., & Foufoula-Georgiou, E. (2015). Landscape reorganization under changing climatic forcing: Results from an experimental landscape. *Water Resources Research*, *51*(6), 4320–4337. https://doi.org/10.1002/2015WR017161

Smith, D., Newman, W., Watson, F., & Hameister, J. (2004). Physical and hydrologic assessment of the Carmel River watershed, California. Report to Carmel River watershed conservancy. Watershed Institute, California State University Monterey Bay, Report No. WI-2004-05/2 (p. 94). Retrieved from http://ccows.csumb.edu/pubs/reports/CCoWS_CRWC_CarmAssPhysHyd_041101.pdf

Smith, D. P., Kvitek, R., Aiello, I., Iampietro, P., Quan, C., Paddock, E., et al. (2009). *Fall 2008 stage-volume relationship for Los Padres reservoir, Carmel valley, California: Prepared for the Monterey Peninsula water management District* (p. 30). The Watershed Institute, California State University Monterey Bay, Publication no. WI-2009-2.

Smith, D. P., Kvitek, R., Iampietro, P., & Consulo, P. (2018). *Fall 2017 stage-volume relationship for Los Padres reservoir, Carmel River, California. Report prepared for the Monterey Peninsula water management District* (p. 21). Watershed Institute, California State University Monterey Bay, Publication no. WI-2015-05. Retrieved from http://ccows.csumb.edu/pubs/reports/CCoWS_MPWMD_LosPadres_StageVol_2017_Revised180525.pdf

Smith, D. P., Schneiders, J., Marshall, L., Melchor, K., Wolfe, S., Campbell, D., et al. (2021). Influence of a post-dam sediment pulse and post-fire debris flows on steelhead spawning gravel in the Carmel River, California. *Frontiers in Earth Science*, *9*, 802825. https://doi.org/10.3389/feart.2021.802825

Snyder, N. P., Wright, S. A., Alpers, C. N., Flint, L. E., Holmes, C. W., & Rubin, D. M. (2006). Reconstructing depositional processes and history from reservoir stratigraphy: Englebright Lake, Yuba River, northern California. *Journal of Geophysical Research*, *111*(F4), F04003. https://doi.org/10.1029/2005JF000451

Spigel, K. M., & Robichaud, P. R. (2007). First-year post-fire erosion rates in Bitterroot national forest, Montana. *Hydrological Processes*, *21*(8), 998–1005. https://doi.org/10.1002/hyp.6295

State of California. (2018). California's fourth climate change assessment. Retrieved from http://www.climateassessment.ca.gov/state/docs/20180827-StatewideSummary.pdf

Swain, D. L. (2021). A shorter, sharper rainy season amplifies California wildfire risk. *Geophysical Research Letters*, *48*(5), e2021GL092843. https://doi.org/10.1029/2021GL092843

Swain, D. L., Langenbrunner, B., Neelin, J. D., & Hall, A. (2018). Increasing precipitation volatility in twenty-first-century California. *Nature Climate Change*, *8*(5), 427–433. https://doi.org/10.1038/s41558-018-0140-y

Thomas, M. A., Kean, J. W., McCoy, S. W., Lindsay, D. N., Kostelnik, J., Cavagnaro, D. B., et al. (2023). Postfire hydrologic response along the central California (USA) coast: Insights for the emergency assessment of postfire debris-flow hazards. *Landslides*, *20*(11), 2421–2436. https://doi.org/10.1007/s10346-023-02106-7

Thornton, M. M., Shrestha, R., Wei, Y., Thornton, P. E., & Kao, S.-C. (2022). *Daymet: Daily surface weather data on a 1-km grid for north America, version 4 R1*. ORNL DAAC. https://doi.org/10.3334/ORNLDAAC/2129

Thurston, L. L., Schiefer, E., McKay, N. P., & Kaufman, D. S. (2023). Suspended sediment deposition and sediment yields at lake Peters, northeast Brooks range, Alaska: Fluvial and lake-based approaches. *Earth Surface Processes and Landforms*, *48*(13), 2521–2535. https://doi.org/10.1002/esp.5642

Trenberth, K. E. (2011). Changes in precipitation with climate change. *Climate Research*, *47*(1), 123–138. https://doi.org/10.3354/cr00953

U.S. Department of Agriculture. (2016). *Soberanes phase I burned area emergency response Team Report 2500-8* (40 pages). U.S. Department of Agriculture, Forest Service.

U.S. Geological Survey. (1979). Sedimentation study of Los Padres dam—1979 update: Report for Monterey Peninsula water management District (p. 7).

U. S. Geological Survey. (2019). 3D Elevation Program 1-meter resolution digital elevation model. https://www.usgs.gov/the-national-map-data-delivery

U. S. Geological Survey. (2023). National water information system: U.S. Geological survey web interface. https://doi.org/10.5066/F7P55KJN

U.S. Global Change Research Program [USGCRP]. (2023). Fifth national climate assessment. In A. R. Crimmins, C. W. Avery, D. R. Easterling, K. E. Kunkel, B. C. Stewart, et al. (Eds.), U.S. Global Change Research Program. https://doi.org/10.7930/NCA5.2023.CH1

Vieira, D. C. S., Borrelli, P., Jahanianfard, D., Benali, A., Scarpa, S., & Panagos, P. (2023). Wildfires in Europe: Burned soils require attention. *Environmental Research*, *217*, 114936. https://doi.org/10.1016/j.envres.2022.114936

Wagenbrenner, J. W., & Robichaud, P. R. (2014). Post-fire bedload sediment delivery across spatial scales in the interior western United States. *Earth Surface Processes and Landforms*, *39*(7), 865–876. https://doi.org/10.1002/esp.3488

Warrick, J. A., Bountry, J. A., East, A. E., Magirl, C. S., Randle, T. J., Gelfenbaum, G., et al. (2015). Large-scale dam removal on the Elwha River, Washington, USA: Souce-to-sink sediment budget and synthesis. *Geomorphology*, *246*, 729–750. https://doi.org/10.1016/j.geomorph.2015.01.010

Warrick, J. A., East, A. E., & Dow, H. W. (2023). Fires, floods and other extreme events—How watershed processes under climate change will shape our coastlines. *Coastal Futures*, *1*(e2), 1–12. https://doi.org/10.1017/cft.2022.1

Warrick, J. A., Hatten, J. A., Pasternack, G. B., Gray, A. B., Goñi, M. A., & Wheatcroft, R. A. (2012). The effects of wildfire on the sediment yield of a coastal California watershed. *Geological Society of America Bulletin*, *124*(7–8), 1130–1146. https://doi.org/10.1130/b30451.1

Warrick, J. A., Vos, K., East, A. E., & Vitousek, S. (2022). Fire (plus) flood (equals) beach: Coastal response to an exceptional river sediment discharge event. *Scientific Reports*, *12*(1), 3848. https://doi.org/10.1038/s41598-022-07209-0

Westerling, A. L., & Bryant, B. P. (2008). Climate change and wildfire in California. *Climatic Change*, *87*(Suppl. 1), S231–S249. https://doi.org/10.1007/s10584-007-9363-z

Western Regional Climate Center. (2018). Cooperative climatological climate summaries. Retrieved from https://wrcc.dri.edu/Climate/prism_precip_maps.php

Williams, M., Zhang, Y., Estop-Aragonés, C., Fisher, J. P., Xenakis, G., Charman, D. J., et al. (2020). Boreal permafrost thaw amplified by fire disturbance and precipitation increases. *Environmental Research Letters*, *15*(11), 114050. https://doi.org/10.1088/1748-9326-abbeb8

Yanagiya, K., & Furuya, M. (2020). Post-wildfire surface deformation near Batagay, eastern Siberia, detected by L-band and C-band InSAR. *Journal of Geophysical Research: Earth Surface*, *125*(7), e2019JF005473. https://doi.org/10.1029/2019JF005473

Young, H. H., & Hilley, G. E. (2018). Millennial-scale denudation rates of the Santa Lucia mountains, California: Implications for landscape evolution in steep, high-relief, coastal mountain ranges. *Geological Society of America Bulletin*, *130*(11–12), 1809–1824. https://doi.org/10.1130/B31907.1

References From the Supporting Information

Allison, M. A., Kineke, G. C., Gordon, E. S., & Goñi, M. A. (2000). Development and reworking of a seasonal flood deposit on the inner continental shelf off the Atchafalaya River. *Continental Shelf Research*, *20*(16), 2267–2294. https://doi.org/10.1016/s0278-4343(00)00070-4

Draut, A. E., Bothner, M. H., Field, M. E., Reynolds, R. L., Cochran, S. A., Logan, J. B., et al. (2009). Supply and dispersal of flood sediment from a steep, tropical watershed: Hanalei Bay, Kaua'I, Hawai'i, USA. *Geological Society of America Bulletin*, *121*(3–4), 574–585. https://doi.org/10.1130/B26367.1

Draut, A. E., Kineke, G. C., Velasco, D. W., Allison, M. A., & Prime, R. J. (2005). Influence of the Atchafalaya River on recent evolution of the Chenier-plain inner continental shelf, northern Gulf of Mexico. *Continental Shelf Research*, *25*(1), 91–112. https://doi.org/10.1016/j.csr.2004.09.002

Livingston, H. D., & Bowen, V. T. (1979). Pu and ^{137}Cs in coastal sediment. *Earth and Planetary Science Letters*, *43*(1), 29–45. https://doi.org/10.1016/0012-821x(79)90153-5

Nittrouer, C. A., Sternberg, R. W., Carpenter, R., & Bennett, J. T. (1979). The use of Pb-210 geochronology as a sedimentary tool: Application to the Washington continental shelf. *Marine Geology*, *31*(3–4), 297–316. https://doi.org/10.1016/0025-3227(79)90039-2